Government of **Western Australia**
Department of **Mines, Industry Regulation and Safety**

RECORD 2017/12

CONTROLS ON HYDROTHERMAL ALTERATIONS AND GOLD MINERALISATION AT COYOTE DEPOSIT, WESTERN AUSTRALIA

by
H Roll

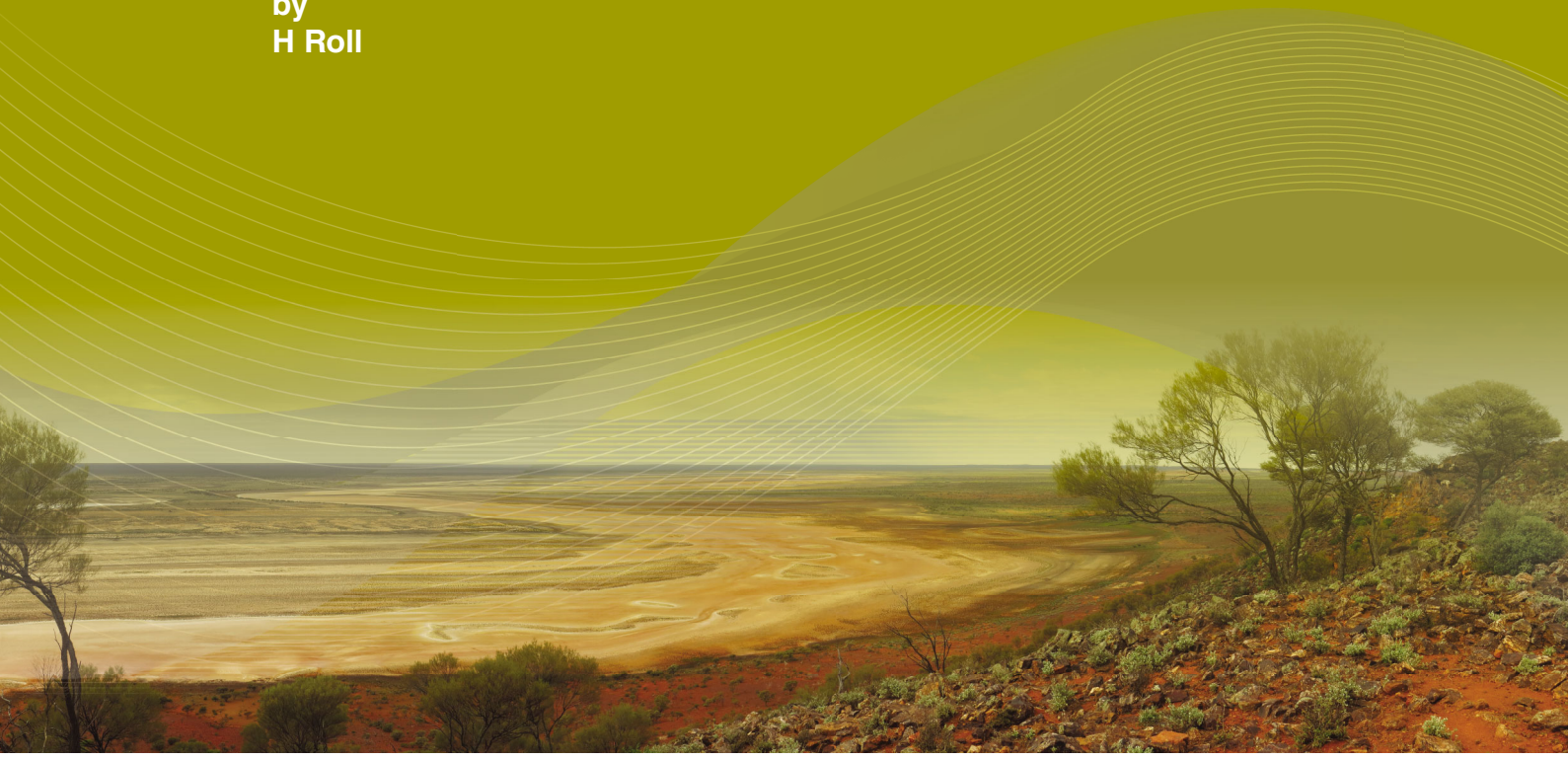

Geological Survey of Western Australia

THE UNIVERSITY OF WESTERN AUSTRALIA

EXPLORATION INCENTIVE SCHEME

Government of **Western Australia**
Department of **Mines, Industry Regulation and Safety**

Record 2017/12

CONTROLS ON HYDROTHERMAL ALTERATIONS AND GOLD MINERALISATION AT COYOTE DEPOSIT, WESTERN AUSTRALIA

by
H Roll

Perth 2017

Geological Survey of Western Australia

REFERENCE
The recommended reference for this publication is:
Roll, H 2017, Controls on hydrothermal alterations and gold mineralisation at Coyote deposit, Western Australia: Geological Survey of Western Australia, Record 2017/12, 44p.

National Library of Australia Card Number and ISBN 978-1-74168-770-5

Grid references in this publication refer to the Geocentric Datum of Australia 1994 (GDA94). Locations mentioned in the text are referenced using Map Grid Australia (MGA) coordinates, Zone 52. All locations are quoted to at least the nearest 100 m.

About this publication
This Record is a Master's thesis researched, written and compiled as part of a collaborative project between the Geological Survey of Western Australia (GSWA) and The University of Western Australia, to investigate the nature of gold mineralisation at the Coyote deposit based on the examination of one diamond drillhole, CYDD0178. Although GSWA has provided field support for this project, the scientific content of the Record, and the drafting of figures, was the responsibility of the author. No editing has been undertaken by GSWA.

Published 2017 by Geological Survey of Western Australia
This Record is published in digital format (PDF) — it and the digital appendix are available online at <www.dmp.wa.gov.au/GSWApublications>.

Further details of geological products and maps produced by the Geological Survey of Western Australia are available from:
Information Centre
Department of Mines, Industry Regulation and Safety
100 Plain Street
EAST PERTH WESTERN AUSTRALIA 6004
Telephone: +61 8 9222 3459 Facsimile: +61 8 9222 3444
www.dmp.wa.gov.au/GSWApublications

Cover image: Elongate salt lake on the Yilgarn Craton — part of the Moore–Monger paleovalley — here viewed from the top of Wownaminya Hill, 20 km southeast of Yalgoo, Murchison Goldfields. Photograph taken by I Zibra for the Geological Survey of Western Australia

Controls on hydrothermal alterations and gold mineralisation at Coyote deposit, Western Australia

Henry ROLL

ID. 21666423

Word Count. 7,005

Supervisors:

Dr. Sandra Occhipinti[1], Dr. Alan Aitken[1], and Dr. Paul Duuring[2]

[1]Centre for Exploration Targeting, School of Earth and Environment, The University of Western Australia

[2]Geological Survey of Western Australia

This thesis is submitted in partial fulfilment of the requirements for a Masters in Geoscience on 17th May 2017

Abstract

Gold mineralisation models in the Granite Tanami Orogen of Australia are debatable. Critical elements like the source of gold-laden fluids, fluids pathways, and depositional sites are not clearly defined. These aspects are addressed in this study through investigations of diamond drill hole CYDD0178 located in Coyote Open Cast Mine. The methods used include conventional logging, interpretation of pre-existing geochemical data, analyses of HyLogger data, and petrographic studies. Data and observations suggest that gold-rich fluids were sourced from reduced magma and country rocks. Magma is the main driver that scavenged gold and other metals from the country rocks. Furthermore, higher grade gold largely corresponds to higher vein density in shear zones. Such spatial associations suggest that the intersection of Gonzales Fault and the Coyote Anticlinal Fold represents damaged high permeability zones suitable for transfer and focusing of auriferous fluids. These structures are the principal controls on gold localisation, and granite emplacement at Coyote. Other controls include competency contrast, bedding, and nature of host rocks. The deposit is characterised by granitoid association, metal zoning comprising Au with elevated Bi-Te-As-Ag-K-Pb-Al assemblage, sheeted parallel, folded, and cross-cutting quartz-tourmaline veins, wide range of gold grade, pyrite-arsenopyrite-pyrrhotite-chalcopyrite-sphalerite-galena phases, and synchronous granite emplacement. Based on the above distinguishing features, this paper contends that Coyote deposit is reduced intrusion-related gold model.

1) Introduction

Gold exploration in greenfields regions requires a sound understanding of the principal controls on ore deposit genesis.

The Paleoproterozoic Granite Tanami Orogen (GTO) constitutes part of North Australian craton and spans the state border between Western Australia and the Northern Territory (Wygralak et al., 2005; Bagas et al., 2008; Joly et al., 2012; Hillyard, 2012). This area is increasingly recognised as one of the major gold provinces in Australia (Huston et al., 2006; Hillyard, 2012), with total resources (including historic output) more than 10 million ounces (Wygralak et al., 2005 and Huston et al., 2007). Genetic models of gold mineralisation in the GTO have evolved following two decades of contemporary exploration in the region (Hutson et al., 2006). Gold mineralisation in the GTO has been defined as driven by intrusion-related processes (Bagas et al., 2008; Huston et al., 2006; Tunks and Cook, 2007). However, it is unclear whether gold was sourced from magmatic fluids or if magmatic fluids reacted with the host rocks to leach gold and other metals out of them to concentrate the metals prior to depositing them. The driver for the magmatic fluids has been suggested to be granitic bodies at depth as there are many granite bodies in the region that are about the same age as the mineralisation (Bagas et al., 2009). Additionally, studies have reported that mineralisation in the region is only associated with quartz veins (e.g. Bagas et al., 2014; Huston et al., 2007). Thus, questions remain as to the mineralisation style at Coyote, including if the deposit developed by vein filling or wall rock replacement or both. Have veins and mineralisation precipitated from metamorphic fluids channelled through the region during fold and faulting events associated with the regional-scale DGTO2?

The central question for this research is: what are the principal controls on hydrothermal alterations and gold mineralisation at Coyote, Western Australia?

This study aims to improve understanding of controls on gold localisation at Coyote deposit and their ensuing exploration implications within the tectonic context of the GTO using high-quality drill hole data.

The objectives of the present study are to delineate the primary and alteration mineralogy; examine structural complexities and their controls on ore genesis; and establish the relative chronology of geologic events at the Coyote gold deposit in Western Australia. The study area forms the western part of the Granite Tanami-Orogen, and is located approximately 220

km south southeast of Halls Creek in the Tanami region, next to the Western Australia-Northern Territory border (Hillyard, 2012), (Refer to Fig. 1).

These objectives are addressed through i) conventional logging, ii) analysis of pre-existing geochemical (assay) data, obtained by Hillyard (2012), iii) HyLogger data analysis, and iv) petrographic analysis of thin sections. The study documents new work on local controls of gold localisation at Coyote, WA, links to alteration assemblages and local structures, and how they correlate with regional structures, and implications for further Coyote-style mineralisation in the GTO.

2) Regional setting

The oldest rocks in the Tanami region are the Archaean ortho-gneisses from the Billabong complex in the Northern Territory (Fig.1), and yield a U-Pb SHRIMP age of 2514 ± 2 Ma on magmatic zircon (Cross and Crispe, 2007; Page et al., 1995). These rocks are unconformably overlain by a thick package of volcano-sedimentary units (Bagas et al., 2010), and subsequently intruded by ca. 1795 Ma granitic rocks (Bagas et al., 2010; Cross and Crispe, 2007; Smith, 2001). The ca. 1864 – 1844 Ma Tanami Group (Blake et al., 1973) includes the Stubbins and Killi Killi Formations in Western Australia (Bagas et al., 2008, 2009, 2010; Joly et al., 2010), are the oldest exposed Paleoproterozoic rocks in the western part of the GTO and comprise thick turbiditic successions of sandstone, siltstone, shale, chert, BIF, and felsic or mafic volcanic rocks (Bagas et al., 2008; Lambeck et al., 2008). This rock package has been folded into anticlinal folds that dip steeply to the south, and 40^0 to the North; and cut by NW – trending reverse faults (Hillyard, 2012).

Goleby et al. (2009) suggest that the earliest structures in the GTO are basin forming ($DGTO_E$) WNW – trending listric crustal-scale faults. These structures have been recognised in the Archaean basement, dipping southward to the Moho discontinuity (Goleby et al., 2009). Further, Joly et al. (2010) assert that the original basin structure of the GTO is deduced as a succession of orogen-parallel normal faults and orogen-transverse transfer faults formed during southward-directed rifting (refer to Fig.2).

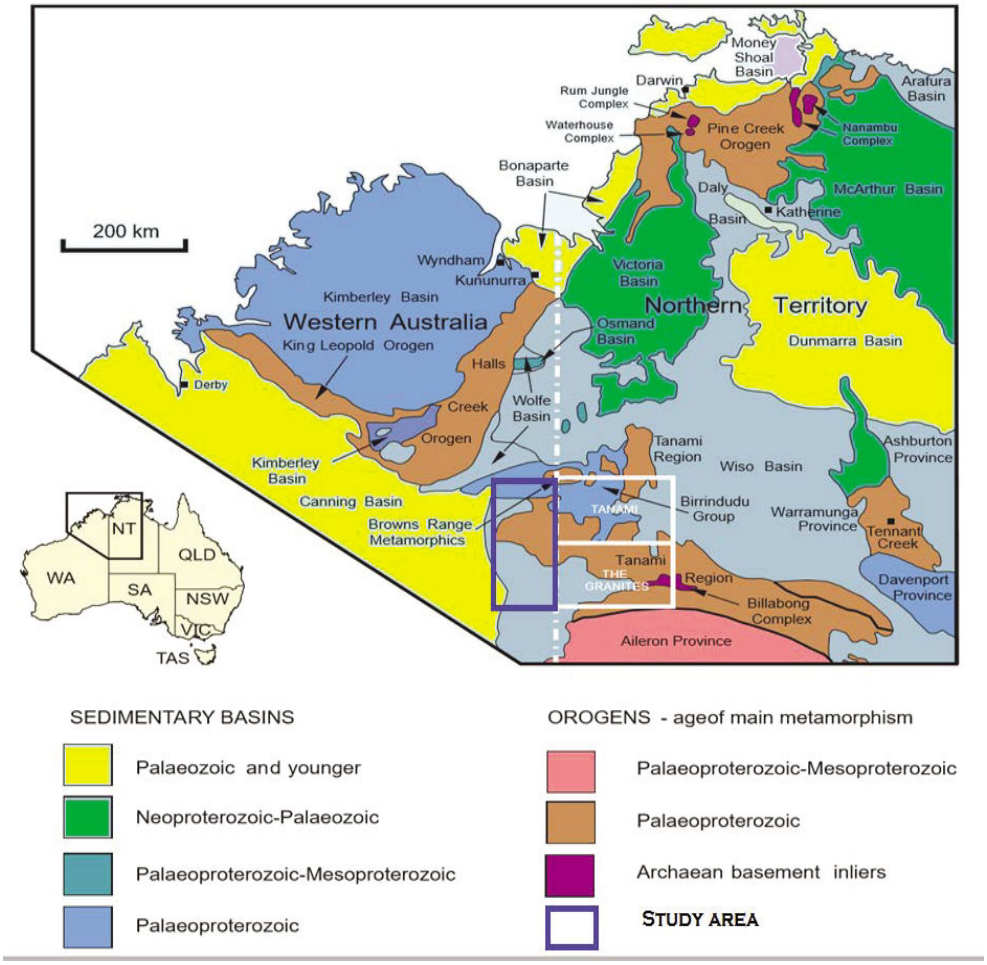

Figure 1. Regional geological setting of Tanami region (modified after Hendricks et al., 2000).

The first deformation event - $DGTO_1$ in WA is characterised by northerly trending isoclinal folds associated with common layer-parallel foliation ($SGTO_1$) that is at an acute angle to bedding at fold hinge zones, and thrust and transpressional faults (Joly et al., 2012). As described by Bagas et al. (2008, 2009), the $DGTO_1$ event is an oblique inversion of the $DGTO_E$ architecture, and is interpreted as a thin-skinned tectonic episode, which formed at ca. 1850 Ma during E-W $DGTO_1$ compression. Structures associated with $DGTO_1$ have been tightly folded and truncated east-southeast and verge to the south in a south-directed $DGTO_2$ compressional event (Bagas et al., 2008, 2009). Both the $DGTO_1$ and $DGTO_2$ deformation episodes are linked to low-grade regional metamorphism (Bagas et al., 2008, 2009).

Based on the above inverted rift model, Joly et al. (2010) contend that the geometry and spatial distribution of granite intrusions in the western GTO are controlled by the combined $DGTO_E$-$DGTO_1$-$DGTO_2$ structures. Given that all granite suites identified at the surface have

been dated at approximately ca. 1795 Ma in age (Bagas et al., 2010), these cross-cutting relationships suggest that the $DGTO_2$ event is broadly synchronous with granite emplacement at ca. 1795 Ma, and that $DGTO_E$ and $DGTO_1$ structures were locally reactivated during this episode (Joly et al., 2010).

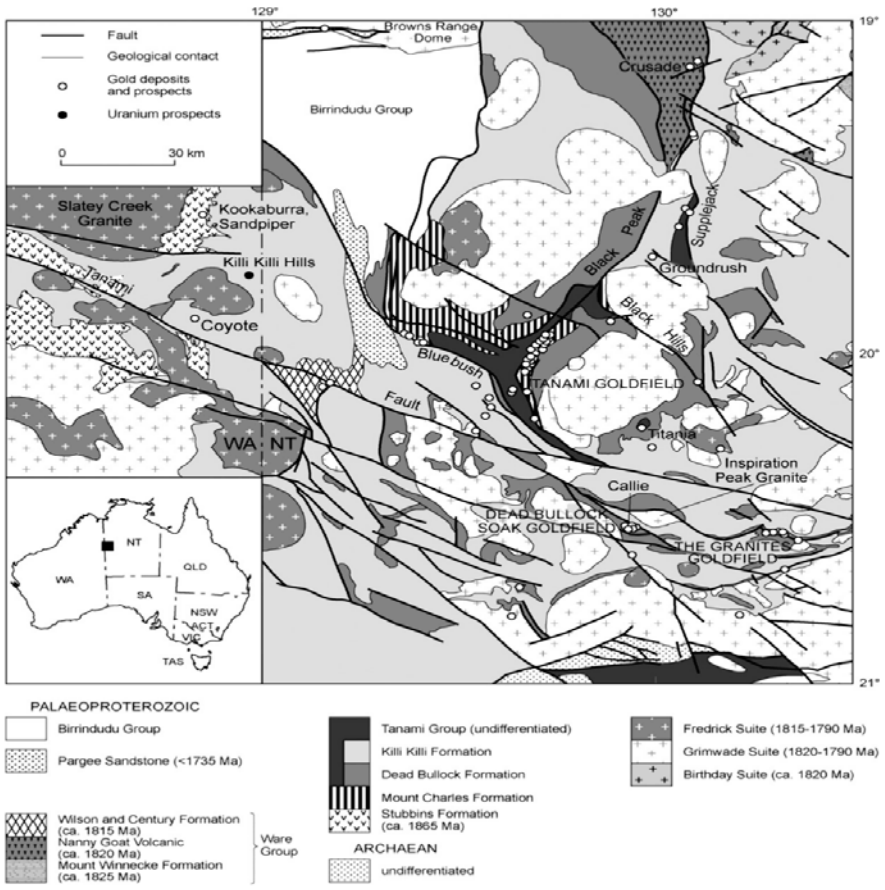

Figure 2. Simplified geology map (after Hutson et al., 2007)

Mineralisation

Hillyard (2012) states that gold mineralisation in the GTO is characterised by different styles and structural settings. Concisely, the deposits occur as high grade quartz veins (Callie, Coyote), high to medium grade stratiform lode style (Bald Hill), high to medium grade shear and fault hosted (The Granites, Tanami, Bald Hill), and high grade quartz veins in brittle dolerite (Groundrush). This has been supported by Bagas et al. (2014), who contend that majority of these deposits are structurally controlled, apart from granite hosted mineralisation at Buccaneer.

These structures provided the pathways and suitable location that allowed pressure drops and focussing of gold bearing fluids into various chemically reactive rocks, localising

high grade mineralisation such as the world-class Callie deposit (e.g. Williams 2007; Huston et al., 2007), Coyote in Western Australia (Bagas et al., 2009), and Groundrush (Huston et al., 2007).

Several models have been proposed to describe gold mineralisation in the GTO by different workers (Bagas et al., 2014). These range from: i) orogenic models linked to ca. 1800 Ma collisional tectonics, and coeval magmatism during late-stage compression (e.g. Griffin et al., 2000; Huston et al., 2007; Pirajno and Bagas 2008); ii) mineralisation within a hornfels zone associated with emplacement of ca. 1825 to 1795 Ma granites (Tunks and Cooke 2007); and iii) synchronous with the earliest deformation episodes (Adams et al., 2007).

Coyote Deposit

The following stratigraphic packages constitute the Tanami Group.

I. The Stubbins Formation

Bagas et al. (2014) define the Stubbins Formation as a package of finely bedded and poorly sorted lithic sandstone, variably ferruginous shale, and a 3m thick banded iron formation consisting of 5–100 mm thick alternating silica-rich and iron-rich meso-bands. The sandstones are characterised by angular to sub-rounded, medium-coarse grained quartz, sericitised and albitised plagioclase feldspar, K-feldspar, detrital muscovite, and chloritized detrital biotite intercalated in a fine-grained matrix of quartz (Bagas et al. 2014). The Killi Killi Formation transitionally overlies the Stubbins Formation as detected from diamond drill hole CYDD0178 (Li et al., 2013; and Bagas et al., 2014). This observation is compatible with the estimated depth of the Stubbins Formation at Coyote as deduced from the reflection seismic data from the study area (Joly et al., 2010). Furthermore, the Stubbins Formation is intruded by a thick succession of fine-medium grained metamorphosed basalt, and dolerite sills at a depth of between 605 and 746 m as seen at CYDD0178 (Bagas et al., 2014).

II. The Killi Killi Formation

Unlike the shale-rich Stubbins Formation, the Killi Killi Formation is sandy and more distinctive of turbidites studied elsewhere in the GTO (e.g. Blake et al., 1979; Boucher and Rossiter, 2010). According to Bagas et al. (2014), the siliciclastic units are primarily fine

grained interbedded shale and medium to coarse grained poorly sorted sandstone containing sub-angular clasts of quartz, feldspar, and mica in a fine-grained matrix of quartz and sericite. Coyote in Western Australia is the only deposit hosted by the Killi Killi Formation, representing about 1% of the discovered gold resources in the GTO.

Mineralisation at Coyote

Gold mineralisation at Coyote is closely linked to the eastward trending inclined, asymmetrical Coyote anticline with the main mineralisation hosted by the steeply dipping Gonzales shear zone (Bagas et al., 2014). The fault is oriented sub-parallel to the axial surface of the anticline and cuts its southern limb (Bagas et al., 2014). Deviations in movement direction including local extensional, reverse and transpressional dextral movement are observed in the fault, suggesting that the fault has been reactivated (Bagas et al., 2014). The Gonzales Fault is interpreted by Hillyard (2012) as the primary pathway for gold laden fluids into the Killi Killi Formation and Coyote deposit. In addition, seismic profiles discussed by Joly et al. (2010, 2012), have provided evidence for existence of crustal-scale intersecting structures beneath this region.

Furthermore, Bagas et al. (2008, 2009) outline that the deposit has been contact metamorphosed and hydrothermally altered, however, it is difficult to recognise this metamorphism and alteration, because the primary detrital mineral suite in the rocks (predominantly quartz, feldspar, muscovite, and biotite) are like the metamorphic and alteration assemblage. Nevertheless, the following alteration styles have been recognised at Coyote: carbonatization, sericitisation, chloritisation, albitisation, and sulfidation (Bagas et al., 2009).

3) Investigations of diamond drill hole CYDD0178

3.1 Conventional logging

In this study, diamond drill hole ID_CYDD0178 was manually logged at one metre spacing to a total drilled depth of 1,206.9m. This investigation aims to delineate rock types, textures,

porosity, weathering intensities, vein density, and proportions of primary and alteration minerals. The drill hole is positioned in the Coyote mine, collar 7796665.5mN 482050.3mE 392.4mRL (MGA Zone 52), and was drilled from the surface at an inclination of -65 (Refer to Fig. 2). This hole was originally planned to penetrate the Stubbins Formation at the interpreted anticline hinge location, and subsequently intersect an underlying granite intrusion at 1000 – 1200 metres below surface as deduced from seismic data (Hillyard, 2012).

Logging of CYDD0178 was done at the Geological Survey of Western Australia's Perth Core Library in Carlisle for two consecutive weeks. The first week involved documentation of various rock types and associated textures, porosity, weathering intensities, and vein densities across the entire drill hole. During the second week, primary and alteration minerals including sulfides were documented.

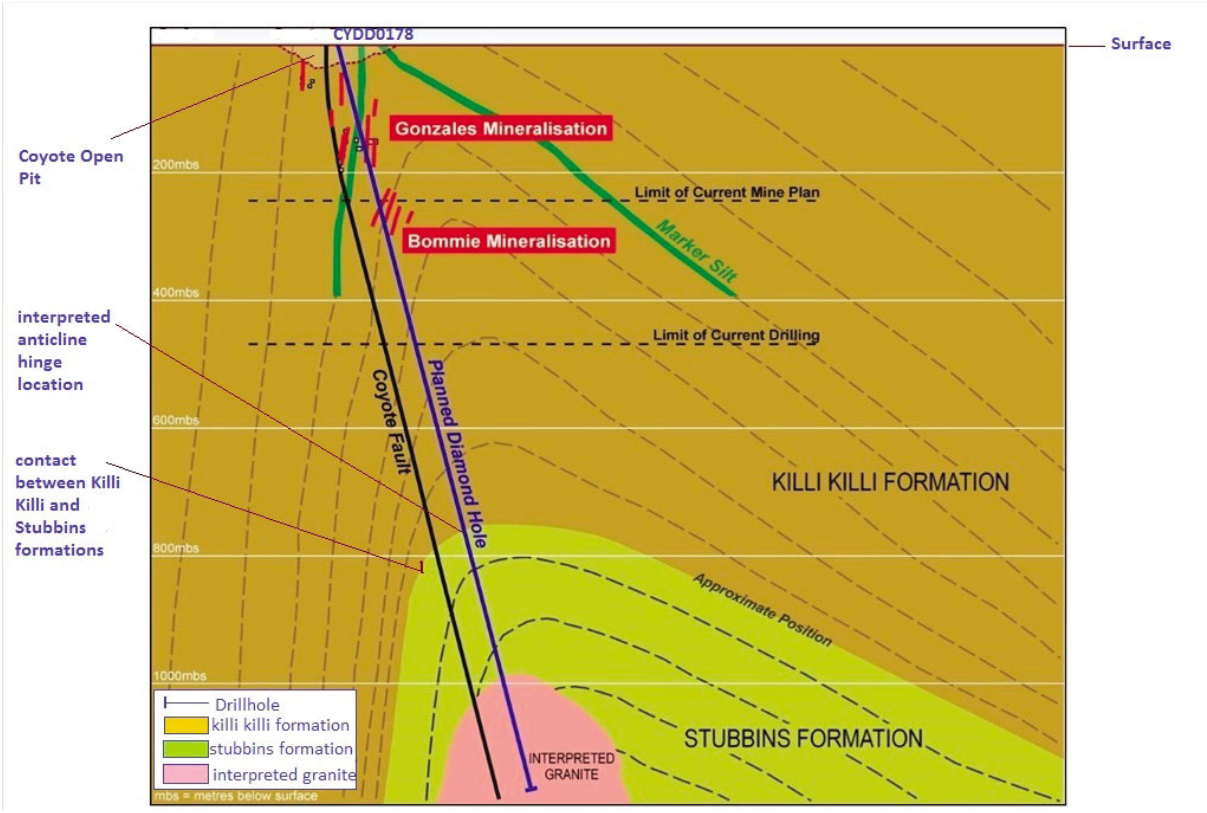

Figure 3. Cross-section through the Coyote open pit, depicting the location of drill hole CYDD0178 and the intersection of major formations by the drill hole (modified after Hillyard, 2012).

I. Rock types

Two major formations of the Tanami Group; the Killi Killi and the Stubbins Formations have been intersected by CYDD0178. The Killi Killi Formation transitionally overlies the Stubbins Formation and comprises five different macrobands that are labelled from top to bottom AKK (601.6 m), BKK (20.8 m), CKK (85.3 m), DKK (9.2 m), and EKK (309.4) m thick. These macrobands constitute the upper and lower portions of the drill core (Refer to Table 1) and make up an apparent 1,026.3m thickness within the total rock package intersected by the drill core. It was found that the Stubbins and Killi Killi Formations are interleaved, and devoid of a simple single contact. Furthermore, AKK, BKK, CKK, DKK, and EKK bands consist predominantly of turbidite sequences that are moderate to heavily veined, and hydrothermally altered. Intense weathering extends from the surface to a depth of nearly 105 m. Below about 105 m, weak to strong weathering extends down to a depth of 400 m. Average grain sizes in the Turbidite sequences generally range from medium to coarse-grained, and are moderately to poorly sorted. Porosity is generally moderate to low in the turbidite units, although it is very low, to non-existent in the mafic units.

The Stubbins Formation, in contrast, consists of eight meso-macrobands labelled as FS (5.9 m), GS (35.6 m), HS (49.7 m), IS (5.9 m), JS (47.05 m), KS (12.85 m), LS (3.9 m), and MS (19.5 m) thick intervals respectively, which form a 180.4 m thick package. These bands consist of sandstones that are intruded by dolerite and gabbro sills. The upper FS band is interpreted here to represent the top of Stubbins Formation (See Table 1), and marks the shift from the sandstone-dominated Killi Killi Formation, to the shale-rich Stubbins Formation. Further down-hole, the MS sandstone layer forms the lower portion of Stubbins Formation and is underlain by Killi Killi Formation at an interpreted depth of about 782 m (Refer to Table 1.). The contact between the KS sandstone layer and 47.05 m thick dolerite sill at a depth of nearly 745.75 m is interpreted here as a contact aureole. Average grain size ranges from medium - coarse to very coarse in the dolerite and gabbro rocks respectively. Weathering is very weak in the sandstone mesobands down the hole whereas the mafic units are unweathered (Refer to Fig. 4).

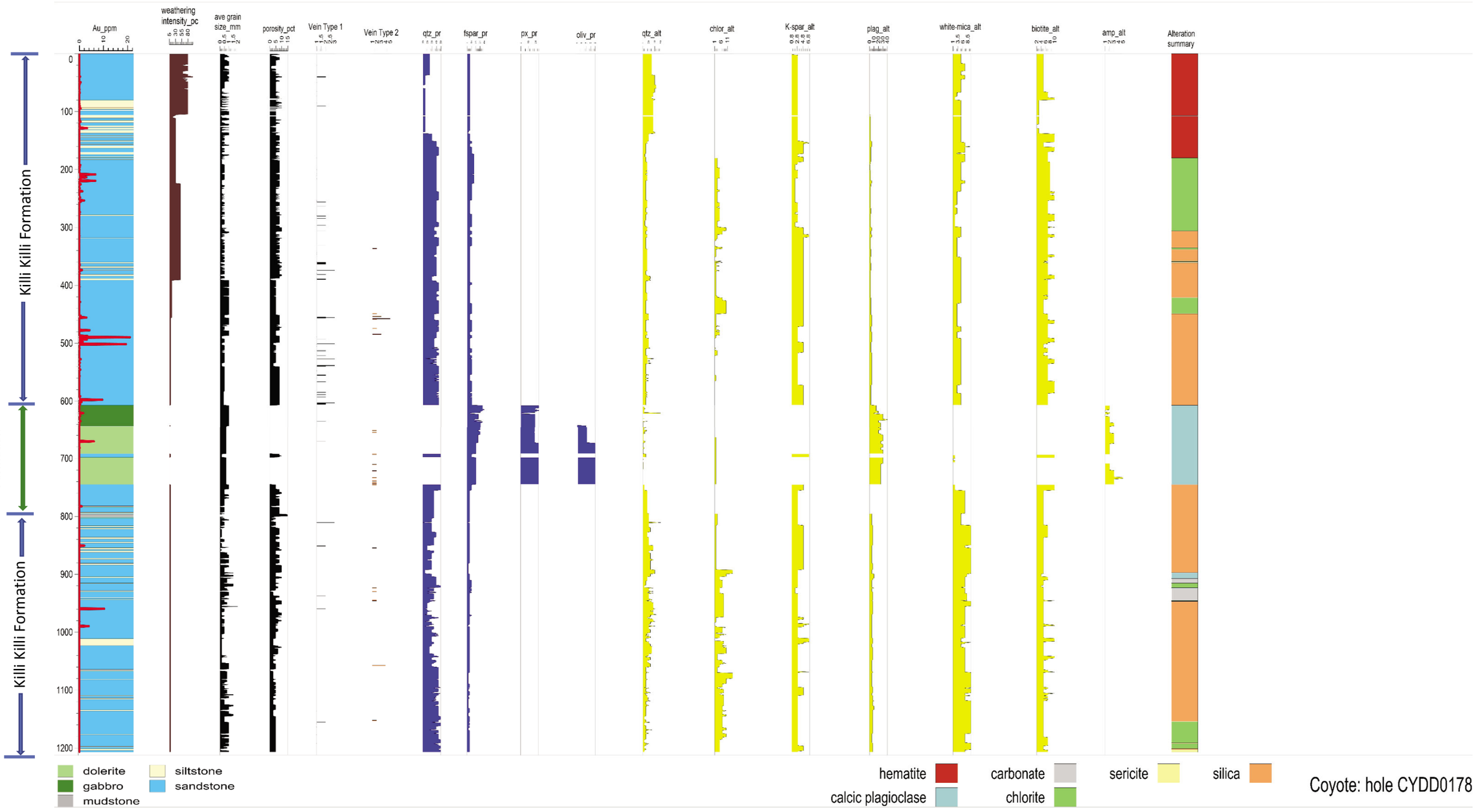

Figure 4. Coyote graphic log CYDD0178.

Table 1. Summary of rock types intersected in CYDD0178

MFrom	MTo	Rock type	Formation	Thickness (m)	Remarks
0	601.6	sandstone & siltstone	Killi Killi	601.6	Alternating beds of sandstone and siltstone, heavily veined.
601.6	607.5	carbonaceous& cherty sediments	Stubbins	5.9	Top of Stubbins Formation – variably ferruginous and carbonaceous cherty beds.
607.5	643.1	gabbro	Stubbins	35.6	Mafic intrusion associated with pyrite, pyrrhotite and arsenopyrite – moderate veining.
643.1	692.8	dolerite	Stubbins	49.7	Ophitic intrusion associated with disseminated pyrrhotite and pyrite – moderate veining.
692.8	698.7	sandstone	Stubbins	5.9	Massive – fine grained sandstone associated with disseminated pyrite.
698.7	745.75	dolerite	Stubbins	47.05	Ophitic mafic sill associated with pyrrhotite and pyrite disseminations, increased carbonatization principally calcite and minor dolomite. Moderate veining.
745.75	758.60	sandstone	Stubbins	12.85	Coarse grained siliciclastic beds, moderately silicified, regularly bedded and increased carbonatization-associated with arsenopyrite.
758.60	762.50	sandstone	Stubbins	3.9	Intensely fractured – shear zone.
762.50	782.0	sandstone	Stubbins	19.5	Medium-grained sandstone layers, interstitial arsenopyrite.
782.0	802.8	Intercalated mudstone, siltstone, & sandstone	Killi Killi	20.8	Intercalations of fractured, very fine mudstone & siltstone, and fine – medium grained sandstone associated with minor dolomite and arsenopyrite.
802.8	888.1	Sandstone & siltstone	Killi Killi	85.3	Silicified and intensely fractured sandstone, and siltstone beds – increased veining and pyrite dissemination.
888.1	897.30	Fault gouge	Killi Killi	9.2	Fault zone
897.30	1206.7	Interbedded sandstone & siltstone	Killi Killi	309.4	Interlayered fine – sandstone and siltstone, variably silicified and fractured, and are associated with disseminated pyrite and large euhedral arsenopyrite – heavily veined and regularly bedded.

II. Primary and alteration mineralogy

i) Primary minerals

The turbidite sequences in the Stubbins and Killi Killi formations are mainly composed of quartz and feldspar, whereas, the mafic units comprise feldspar-pyroxene-olivine assemblages. Unaltered feldspar is relatively more abundant in mafic units than in the turbidites.

ii) Alteration minerals

The main alteration minerals are quartz, white-mica, chlorite, feldspars, biotite, calcite, dolomite, pyrite, arsenopyrite, pyrrhotite, and chalcopyrite. Quartz and feldspar exist in both primary and alteration assemblages in different proportions, making the determination of subtle mineralogical changes difficult.

Four main sulfides have been documented namely pyrite, pyrrhotite, chalcopyrite, and arsenopyrite. These sulfides constitute ± 5% of the rock composition and they occur as euhedral crystals like in the case of pyrite and chalcopyrite and display an igneous texture (Refer to Fig. 6). Majority of these sulfides occur in quartz veins and wall rocks. Type II veins are associated with relatively higher proportions of arsenopyrite.

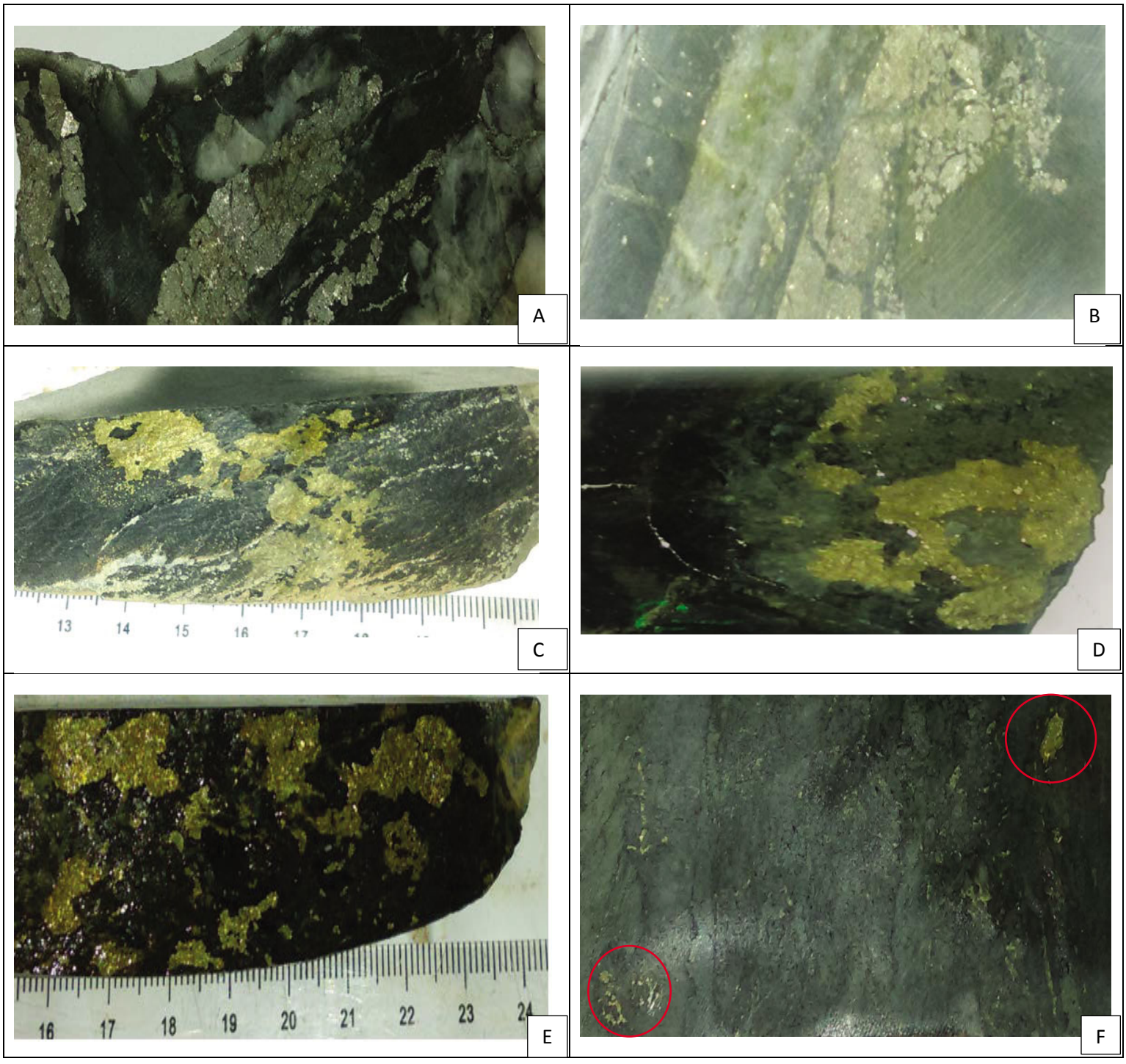

Figure 6 a. Sulfides assemblage a) quartz vein associated with arsenopyrite, b) chloritized bedding parallel quartz vein associated with arsenopyrite, c) wall rock associated with pyrite, d) carbonate quartz vein associated with pyrite e) wall rock associated with euhedral chalcopyrite, and f) disseminated pyrrhotite.

iii) Bedding and Foliation

Structures such as regular/cross-bedding, and foliation characterised the metasedimentary rocks. Bedding has acted as dilatational site along which gold-laden fluids have precipitated (Refer to Fig. 6B). Similarly, foliation has played a role as pathway for hydrothermal fluid flow.

Figure 6 b) cross-bedded sandstone, green circular area display evidence of hydrothermal fluid flow, B) bedded sandstone with pyrite precipitated along lithologic contact, C) intensely foliated sandstone.

iv) Veining

On the bases of their color, morphology, associated mineralogy, and formation mechanism, two broad types of veins have been recognised at Coyote deposit. Vein Type I, is grey quartz and occur in a variety of styles such as single-stage sheeted vein; multi-stage planar, cross-cutting and folded veins (refer to Fig. 7). The grey quartz display alternating bands of white, grey, and green colors, a feature indicative of multiple pulses of fluid generation. Vein Type I, is classified here as the economic vein and are dominantly hosted in the Killi Killi Formation, with moderate occurrences in the Stubbins Formation. Vein assemblage includes quartz ± carbonate (calcite & dolomite) ± chlorite ± sulfides (pyrite, arsenopyrite, pyrrhotite, and chalcopyrite).

There is consensus among different research groups (e.g. Cox et al., 2001; Oliver et al., 2001) that vein type deposits are dilatational sites for gold-rich fluids, created as a consequence of interactions between deformation, metamorphism, and magmatism. In essence, vein type deposits are products of hydrothermal activity triggered by either metamorphism, deformation magmatism. Accordingly, Vein Type 1 are bedding parallel, and is interpreted to have been formed during the second deformation stage ($DGTO_2$) because of rheological difference between the brittle sandstone beds, and the incompetent siltstone layers, creating dilatational zones suitable for transfer and precipitation of gold-bearing fluids (Bagas et al., 2014).

Type I veins are further sub-divided into Type I-A, and Type I-B. Vein Type I-A, is the earlier formed vein set that has been intersected by the later Vein Type I-B, forming a cross-cutting structure (refer to Fig.7b and C). Such cross-cutting relationships indicate that, constant differential movement during the second deformation event-$DGTO_2$, appeared to have created fractures in the early formed Type I-A Veins, which were eventually filled with quartz resulting in the generation of Vein Type I-B.

Vein type II, is milky or bucky quartz, and is characteristically associated with euhedral arsenopyrite. These veins are barren although they contain considerable amount of arsenopyrite. The bucky quartz ranges from few cm to almost one meter in length, and is mainly associated with calcite and dolomite.

Bagas et al. (2009; 2014) propose that the formation of barren quartz veins assigned here as Vein type II, is linked to the late regional deformation event-$DGTO_3$. The late deformation event is associated with NNW-SW shortening resulting in open folds that plunge moderately to the N-NE. However, it is not clear as to why Type II veins are barren.

One likely explanation is because the $DGTO_3$ event is not synchronous with mineralisation and magmatic events at ca. 1795 Ma. As previously mentioned, mineralisation in Coyote is coeval with the $DGTO_2$ and magmatic events, and since Type I Veins are linked to $DGTO_2$ episode, it is probably linked to the magmatic event as well, given that both events are synchronous. Although direct evidence of magmatic origin is lacking, timing relationship is probably a good indicator of magmatic input at Coyote deposit. Magmatism could have acted as energy source that drives the system, and as source of auriferous fluids released during cooling. It is argued here that the gold bearing fluids were contributed from two basic sources; i) fluids released during magmatic differentiation, and ii) country rock. During metamorphic devolatisation, gold was probably leached from the host rock, concentrated, and deposited in Type I veins, leading to depletion in gold content of the country rock. Subsequently, $DGTO_3$ event which is associated with barren (Type II) veins occurred after the host rocks gold content has been depleted. Otherwise, if gold were to be present in the host rock, in conjunction with auriferous fluids released from magma, the $DGTO_3$ event could have resulted in remobilisation and concentration of significant amount of gold into Type II veins.

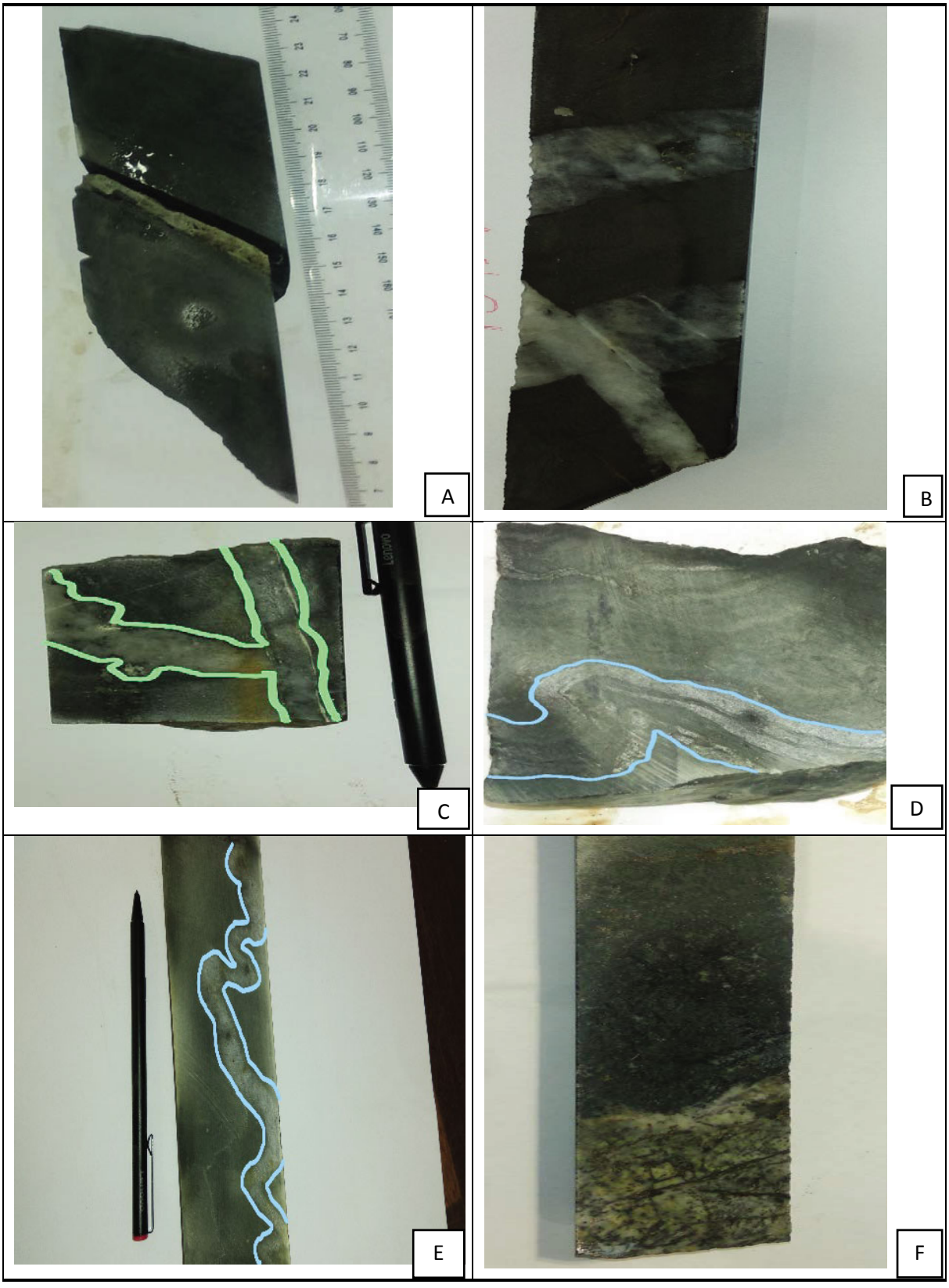

Figure 7a. Vein styles Type 1 A) bedding parallel vein B & C) bedding parallel planar vein and two different generations of intersecting veins D) siltstone-hosted folded vein E) sandstone-hosted folded, vein and F) sandstone-hosted chloritized vein displaying fibrous texture.

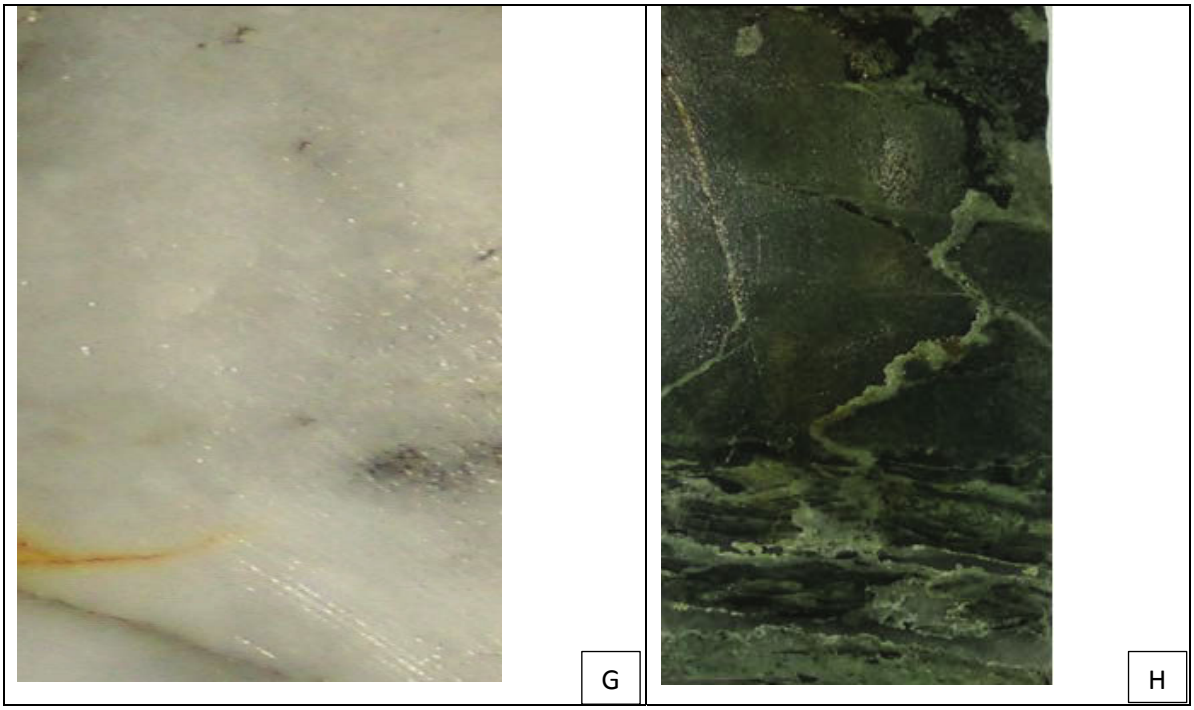

Figure 7 b. Vein Type II g) Bucky quartz vein, h) Fracture - filled milky quartz.

i) Gold anomalies and structures

This analysis attempts to investigate structural controls on gold localisation at Coyote deposit by examining spatial relationships between gold grade and structures such as fold and fault. The method used here is typical to that by Ridley and Mengler (2000) in which the spatial association between major faults and the orebodies were determined by measuring vein density on a typical 29 level of the Charlotte Deeps orebody and linking it to gold grade. In the same way, vein density was measured on a typical level of one metre interval of the Coyote diamond drill hole, for comparison with gold grade (See Fig. 8).

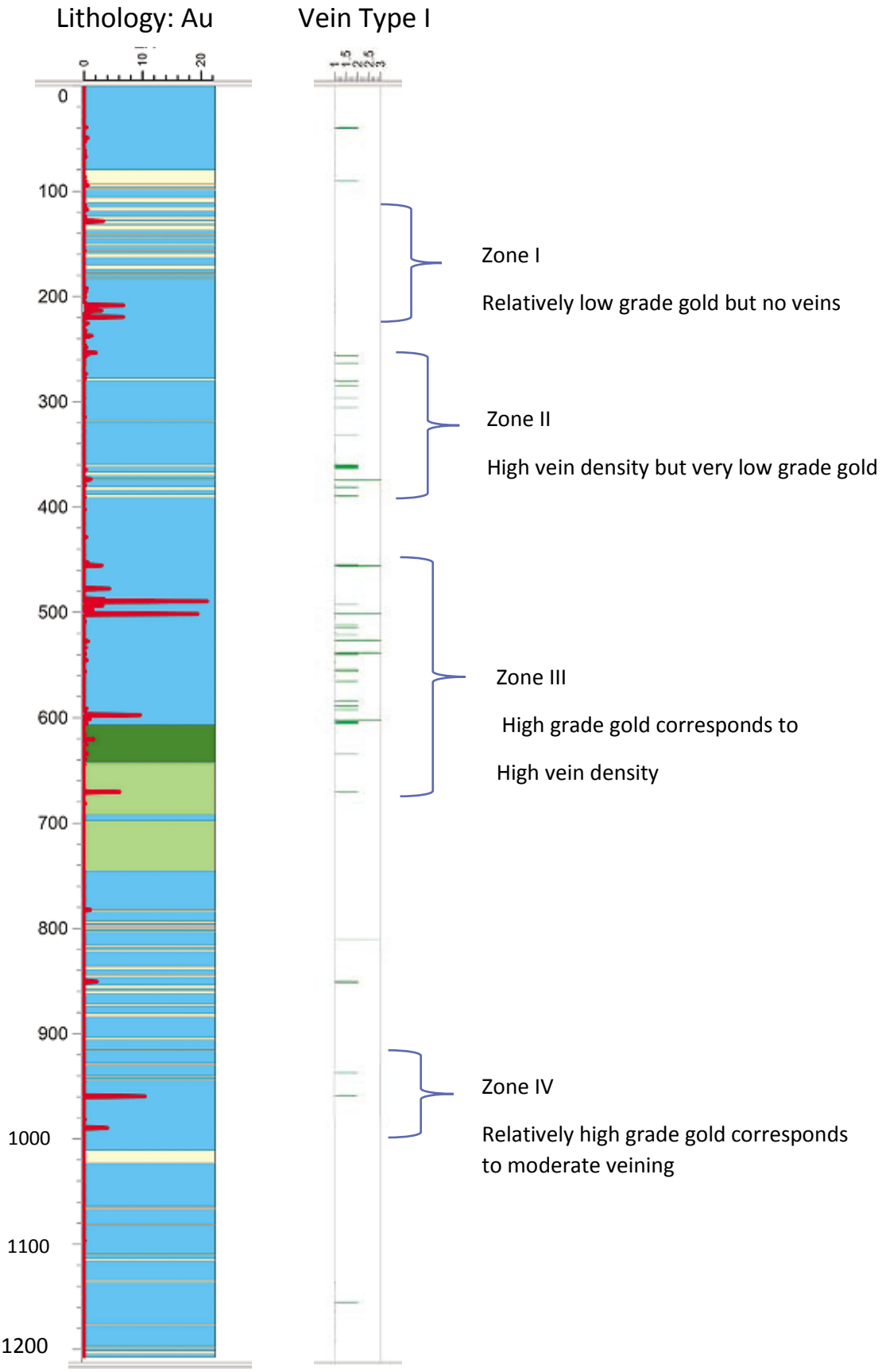

Figure 8. Integrated Lithology and Au grade log versus Type I Veins.

The spatial associations between gold grade and vein density have been divided into four different zones down-hole: Zone I, Zone II, Zone III; and Zone IV (Refer to Fig.8). Zone I display relatively moderate gold grade but devoid of veins. This Zone is deduced here as zone of supergene (secondary) enrichment given that it is located at relatively shallow depth. Zone II, on the other hand, is characterised by significantly high vein density but very low to non-existent gold grade. Comparatively, Vein densities; strongly corresponds to higher gold grade in Zone III, at 489m to 503m interval. Precisely, this zone hosts 21.025 ppm of gold at 489 to 490m depth interval, and 19.407 ppm at 501m to 503m respectively. However, these values drop abruptly to 1.653 ppm and 6.08 ppm down the hole from 620 to 621 metres in the gabbro sill, and 670 to 671 metres in the dolerite units, corresponding to an interval of moderate veining. Similarly, vein density is high in Zone IV, between 959 to 960m, and 989 to 990 m intervals, where two Veins Type I (a) and Type I (b) cross-cut each other. This interval displays relatively higher gold grade of 10.385 ppm and 3.984 ppm respectively. Clearly, gold grade largely corresponds to vein density, suggesting that mineralisation style is vein/fracture-filling.

3.2 Geochemical data processing and analysis

Pre-existing assay data was downloaded from the GSWA online library as part of the A093910_Coyote deeps diamond hole final report. As described by Hillyard (2012), the data was analysed from the whole length of CYDD0178 which was cut and sampled at nominal one metre spacing. The half core was analysed for gold by fire assay with atomic absorption finish at Genalysis Laboratory in Perth, WA. Additionally, intervals of gold mineralisation (i.e. greater than 0.2g/t) were also analysed for a set of 30 elements (Ag, As, Al, Ba, Bi, Ca, Cd, Ce, Co, Cr, Cu, Fe, K, La, Mg, Mn, Mo, Na, Ni, P, Pb, Sb, Sc, Sr, Te, Ti, TI, V, W, Zn) by Aqua regia digest with ICP-OES finish (Hillyard, 2012).

Here, the assay data was analysed in conjunction with Coyote graphic log to determine the relationships between i) gold anomalies and associated trace elements, and ii) gold grade and the nature of corresponding host rocks.

Secondly, the geochemical data was integrated with petrographic data to validate primary and alteration mineral assemblages delineated via HyLogger data and conventional core logging. Green et al. (2010) suggest that results obtained through spectral studies can be validated and confirmed using independent data such as geochemistry and petrography.

I. Gold anomalies and pathfinders

A multivariate statistical analysis like that by Nude et al. (2012) was applied on the geochemical data to delineate pathfinder elements. The analysis concentrates on seven elements, namely As, K, Ag, Pb, Bi, Te and Al respectively. The selection was based on correlation coefficient values for each paired combination of selected variables using ioGAS program.

Christie et al. (2003) observe that analyses of certain geochemical elements and ratios could greatly support exploration for vectoring towards mineralisation zones. Elevated concentrations of K, S, As, and Sb and depletion of Na (as Na/Al) are key pathfinders to ore zones that are easily evaluated by geochemical analysis (Christie et al., 2003).

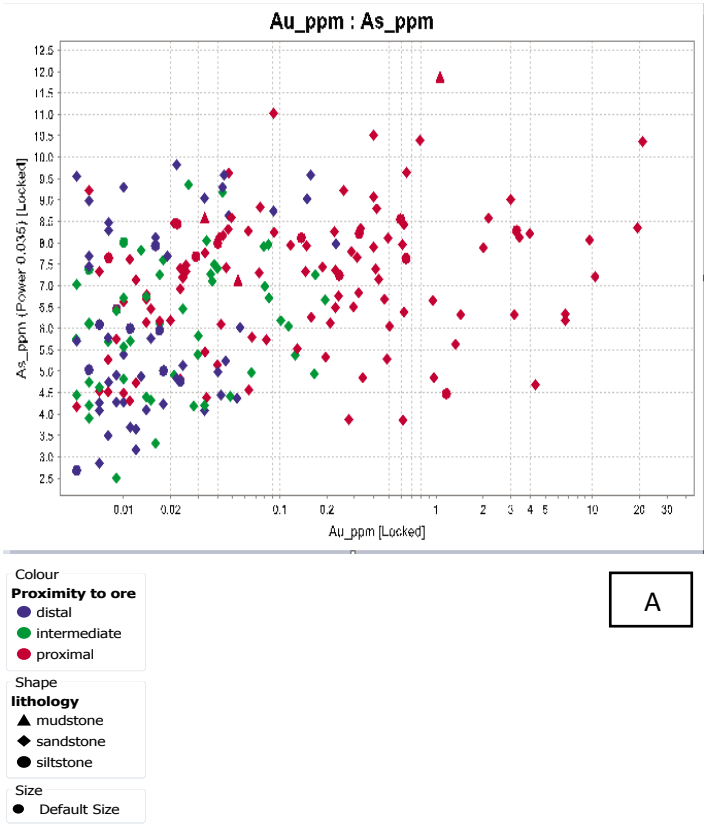

A

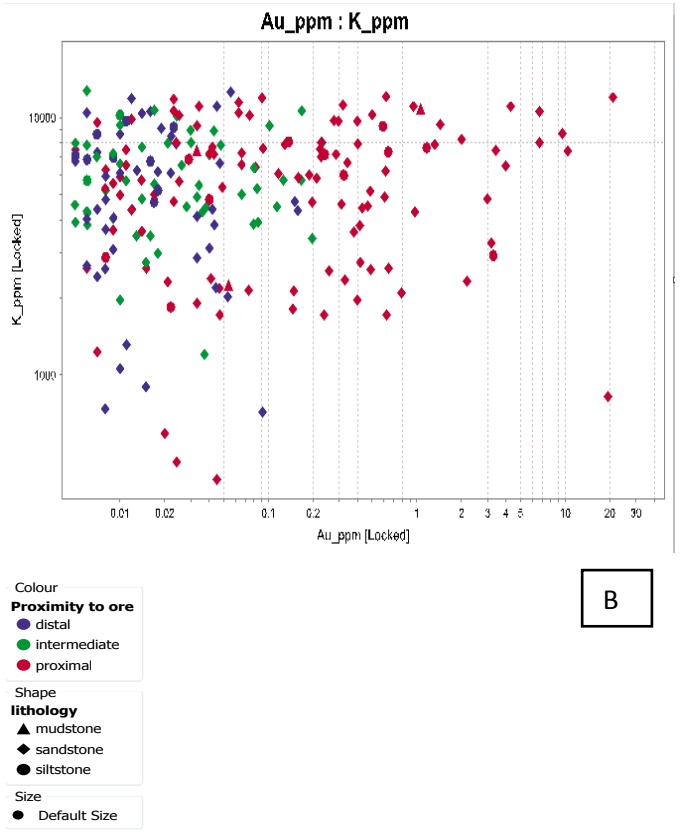

B

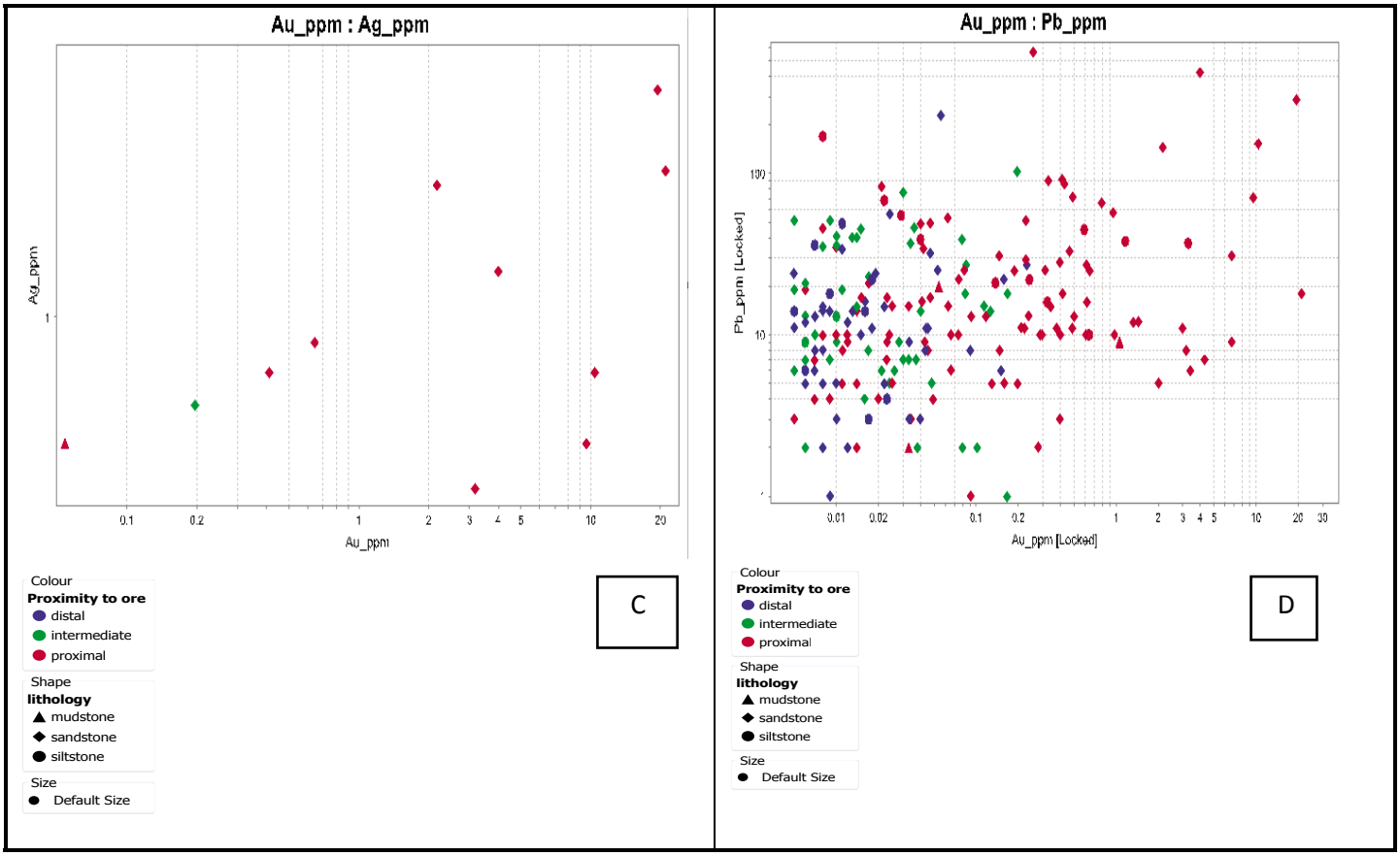
Au_ppm : Ag_ppm
Ag_ppm
Au_ppm
0.1
0.2
1
2
3
4
5
10
20
Colour
Proximity to ore
distal
intermediate
proximal
Shape
lithology
mudstone
sandstone
siltstone
Size
Default Size
C
Au_ppm : Pb_ppm
Pb_ppm [Locked]
Au_ppm [Locked]
100
10
0.01
0.02
0.1
0.2
1
2
3
4
5
10
20
30
Colour
Proximity to ore
distal
intermediate
proximal
Shape
lithology
mudstone
sandstone
siltstone
Size
Default Size
D

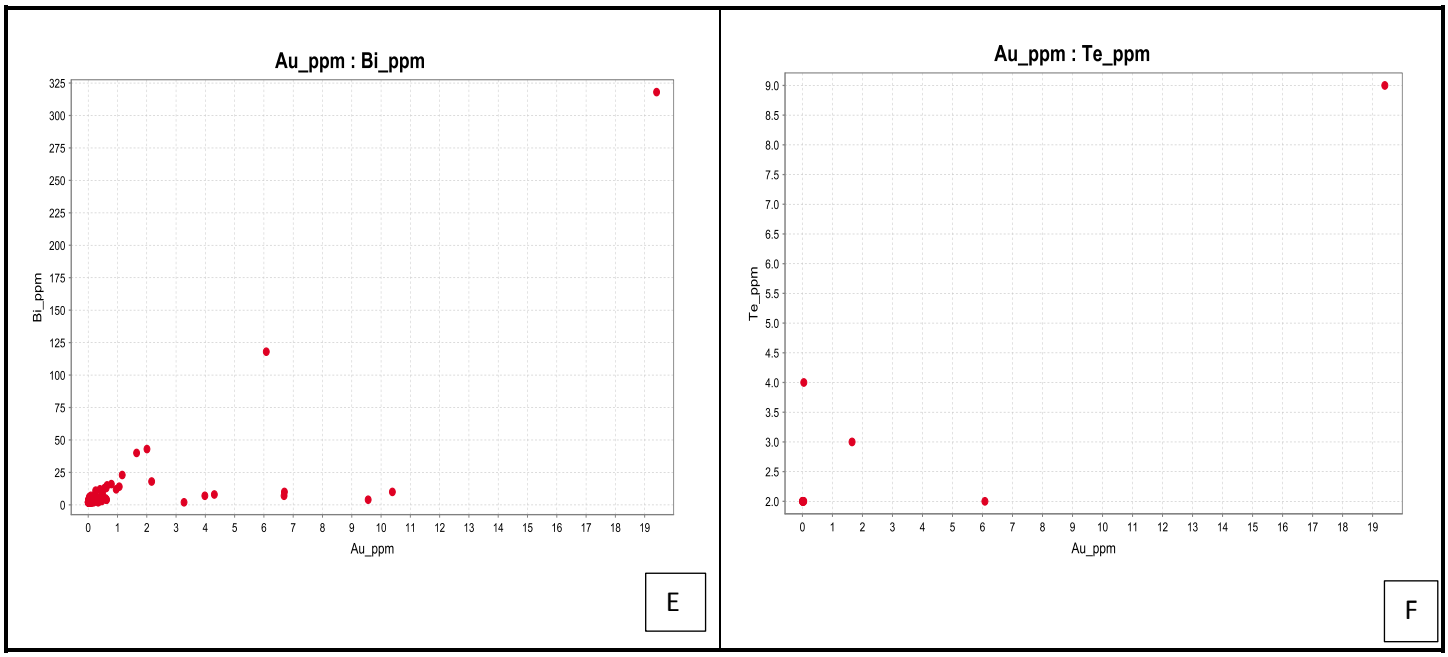
Au_ppm : Bi_ppm
Bi_ppm
Au_ppm
E
Au_ppm : Te_ppm
Te_ppm
Au_ppm
F

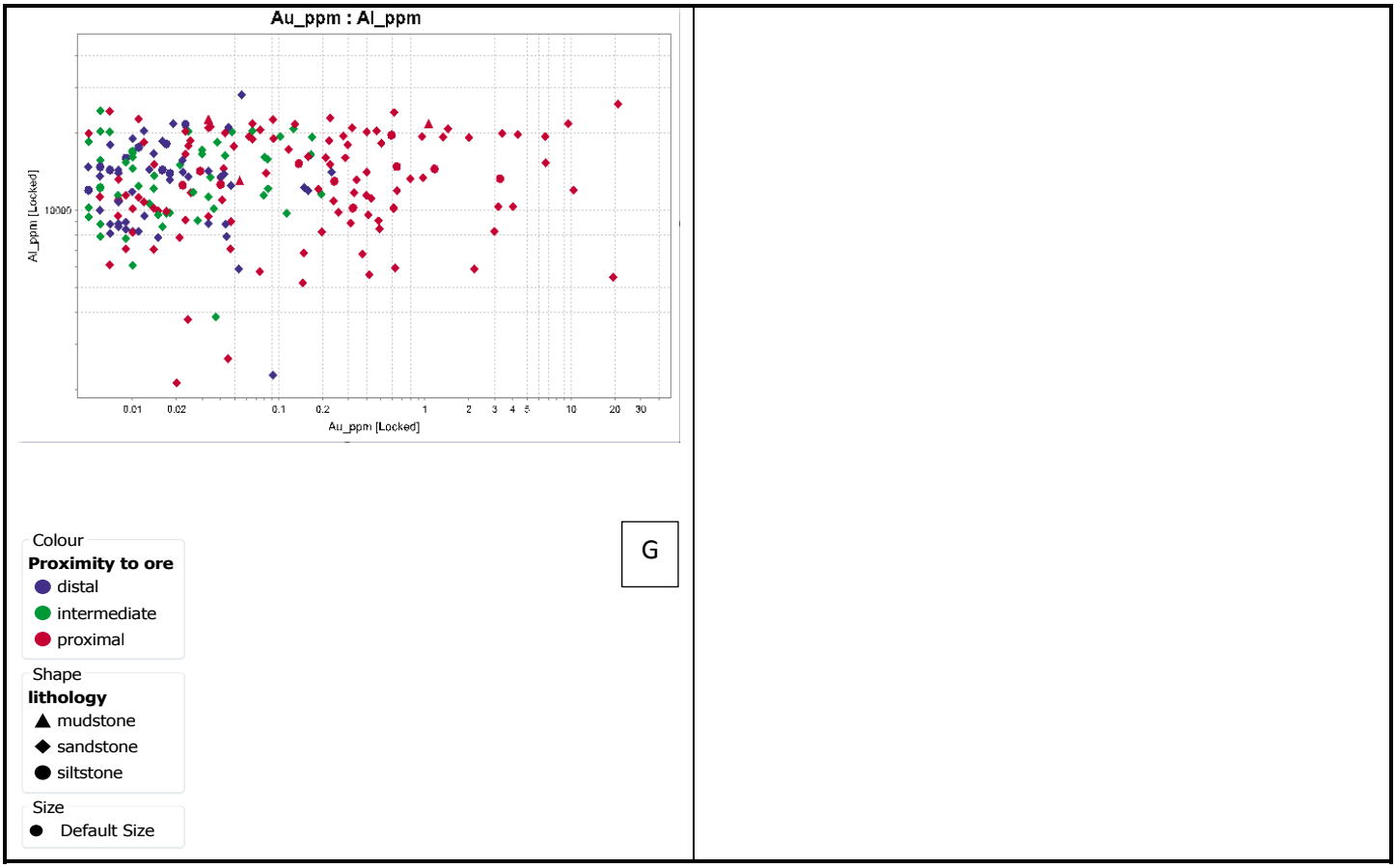

Figure 9. (a, b, c, d, e, f, and g) illustrates plots of gold grade versus associated elements in ppm as follows; As, K, Ag, Pb, Bi, Te & Al respectively.

II. Gold anomalies and favourable host rocks

A log normal distribution analysis was performed on the assay data by plotting gold concentration versus sandstone, siltstone, dolerite, and gabbro, to identify the most favourable host rocks in the stratigraphic sequence.

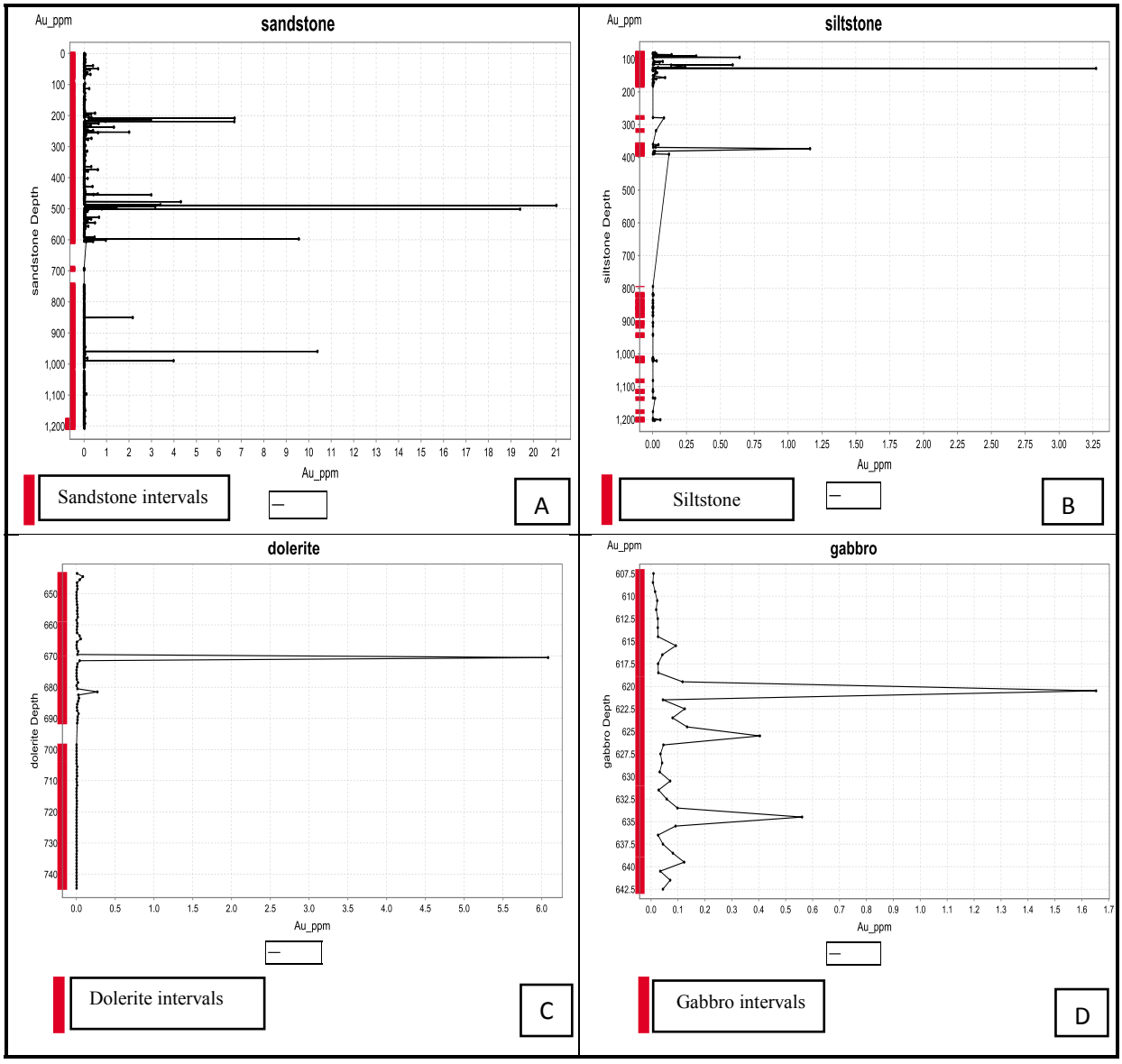

Figure 10. Shows plots of gold grade versus: a) sandstone, b) siltstone, c) dolerite and c) gabbro host rocks

A concise summary of analytical results is presented in Table (4) below.

Table 4. Host rock favourability and corresponding stratigraphic intervals

Host rock	Gold anomaly (ppm)	Stratigraphic interval (m)
Sandstone	19.407 – 21.023	489 – 503
Siltstone	1.162 – 3.273	373 – 374 & 128 - 129
Gabbro	1.653	620 - 621

Dolerite	6.081	670 - 671

Obviously, high grade gold in the range of 19.407 ppm to 21.023 ppm is hosted in sandstone units. Comparatively, gold grade in siltstone beds ranges from 1.62 ppm to 3.273 ppm. The mafic units, on the other hand, display high gold grade of 6.081 ppm in the dolerite, and only 1.653 ppm in gabbro (See Figures 10 c and 10 d). Precisely, analytical results have shown that sandstone and dolerite are the most favourable host rocks at Coyote, whereas, mudstone and gabbro are least favoured for mineralisation.

3.3 HyLogger data processing and analysis

Hyperspectral measurements (SWIR-TIR) were conducted on CYDD0178 using the HyLogging system at the GSWA core library in Perth. Hancock and Huntington (2010), describe HyLogging as a set of modern systems developed by CSIRO that uses rapid reflectance spectroscopy to identify variety of mineral groups including oxides, carbonates, and silicates. One of the drawbacks of this system is its incapability to detect sulphides. However, sulphide abundance in this study is determined via manual logging and petrographic studies.

SWIR and TIR spectral signatures were processed in The Spectral Geologist (TSG®) Pro-mineral analysis software. The Multiple Feature Extraction technique (Cudahy et al., 2008; Laukamp et al., 2010), was used to derive mineral abundance information.

Clark and Roush (1984), emphasise the use of mineralogical diagnostic absorption features for minerals identification. In major rock-forming minerals such as silicates, diagnostic absorption features are in the Short Wave Infra-Red (SWIR) and Thermal-infra-red (TIR) wavelengths (Clark and Roush, 1984). As outlined by Duuring et al. (2017), the spectral signatures of minerals in the SWIR wavelength are directly linked to physiochemistry of the investigated material, whereas, in the TIR wavelength, the spectral signature is also strongly influenced by grain size, emissivity, and optical properties.

Two types of spectral graphic logs were generated to characterise mineral abundances using the SWIR and TIR wavelengths (See Figures. 11a, and 11b). Apart from sulfides, this study concentrates on alteration assemblages that are genetically related to gold mineralisation as

indicated by conventional logging. The subsequent spectral graphic logs were combined with manual graphic logs for comparison.

I. Alteration minerals identified via Short-Wave Infra-Red (SWIR) wavelength.

In this investigation, it was found that the metasedimentary rocks (sandstone, siltstone, and mudstone) is characterised by relative enrichments in Fe-rich chlorite, muscovite, phengite, tourmaline, and lower biotite and calcite abundances. However, epidote, actinolite, tremolite, and hornblende assemblage is rare to non-existent in the metasedimentary units (See Figure 11a.). Mafic igneous dolerite and gabbro, on the other hand, exhibit enrichment in Mg-rich and FeMg-rich chlorite, biotite, epidote, actinolite, tremolite, actinolite, hornblende, phlogopite, serpentinite and moderately higher proportions of calcite (Refer to Figure 11a), and absence of phengite, muscovite, Fe-rich chlorite, and tourmaline.

II. Alteration minerals identified via Thermal Infra-Red (TIR) wavelength.

In the thermal infra-red region, the spectral signatures of metasedimentary rocks exhibit relative enrichments in quartz, muscovite, albite, tourmaline, hematite, and lower biotite, chlorite, and calcite abundances (See Figure 11 b.). These rocks are devoid of epidote, actinolite, hornblende, and augite. Comparatively, dolerite and less commonly gabbro in the TIR display enrichment in biotite, epidote, actinolite, hornblende, prehnite, augite, and calcite. However, these rocks exhibit low quartz content except in the veins; low albite abundance, and rare tourmaline and hematite (Refer to Figure 11 b.).

Based on the above results, two alteration assemblages have been summarised. The first assemblage comprises quartz-muscovite-Fe-rich chlorite-phengite-albite and minor proportions of biotite-tourmaline-hematite and calcite. The second assemblage consists of quartz-Mg-FeMg-chlorite-biotite-phlogophite-epidote-actinolite-hornblende and minor proportions of albite, prehnite, and calcite.

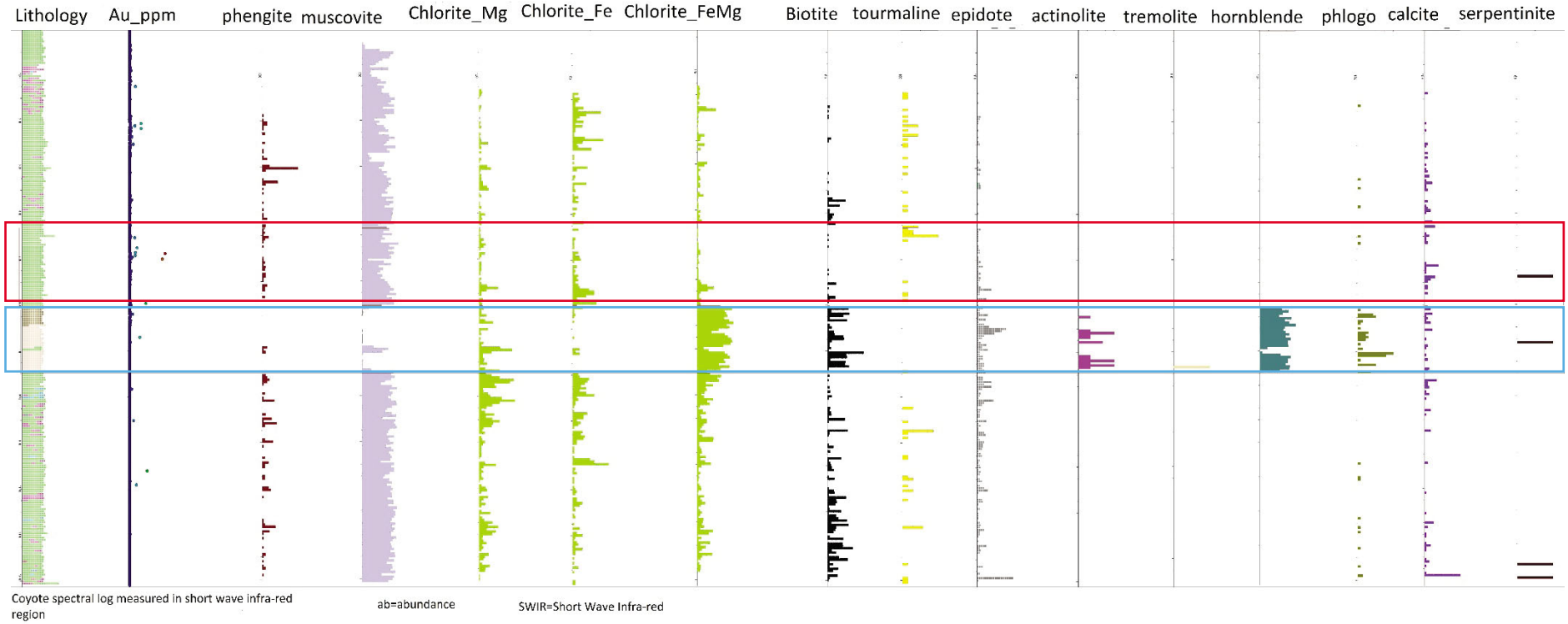

Figure 11 a) Coyote spectral log measured in the SWIR.

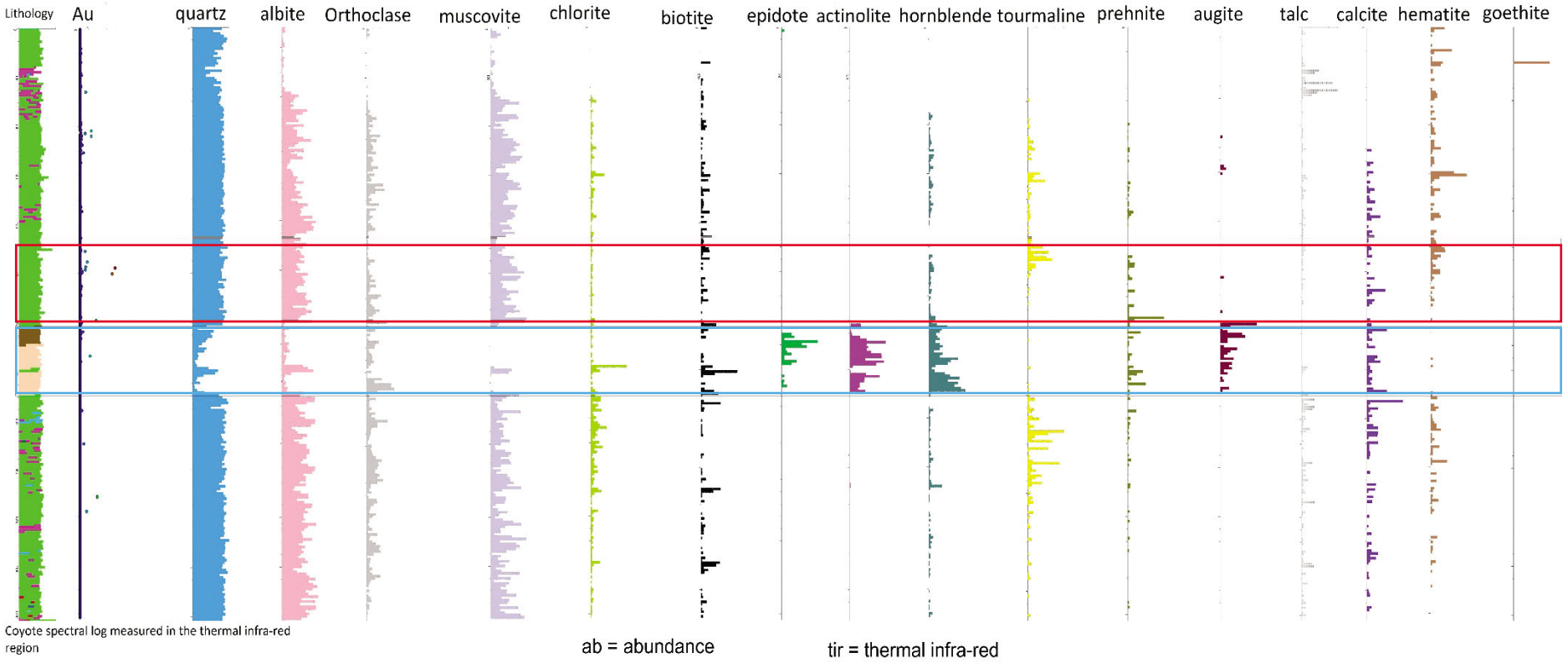

Figure 11 b) Coyote spectral log measured in the thermal infra-red region.

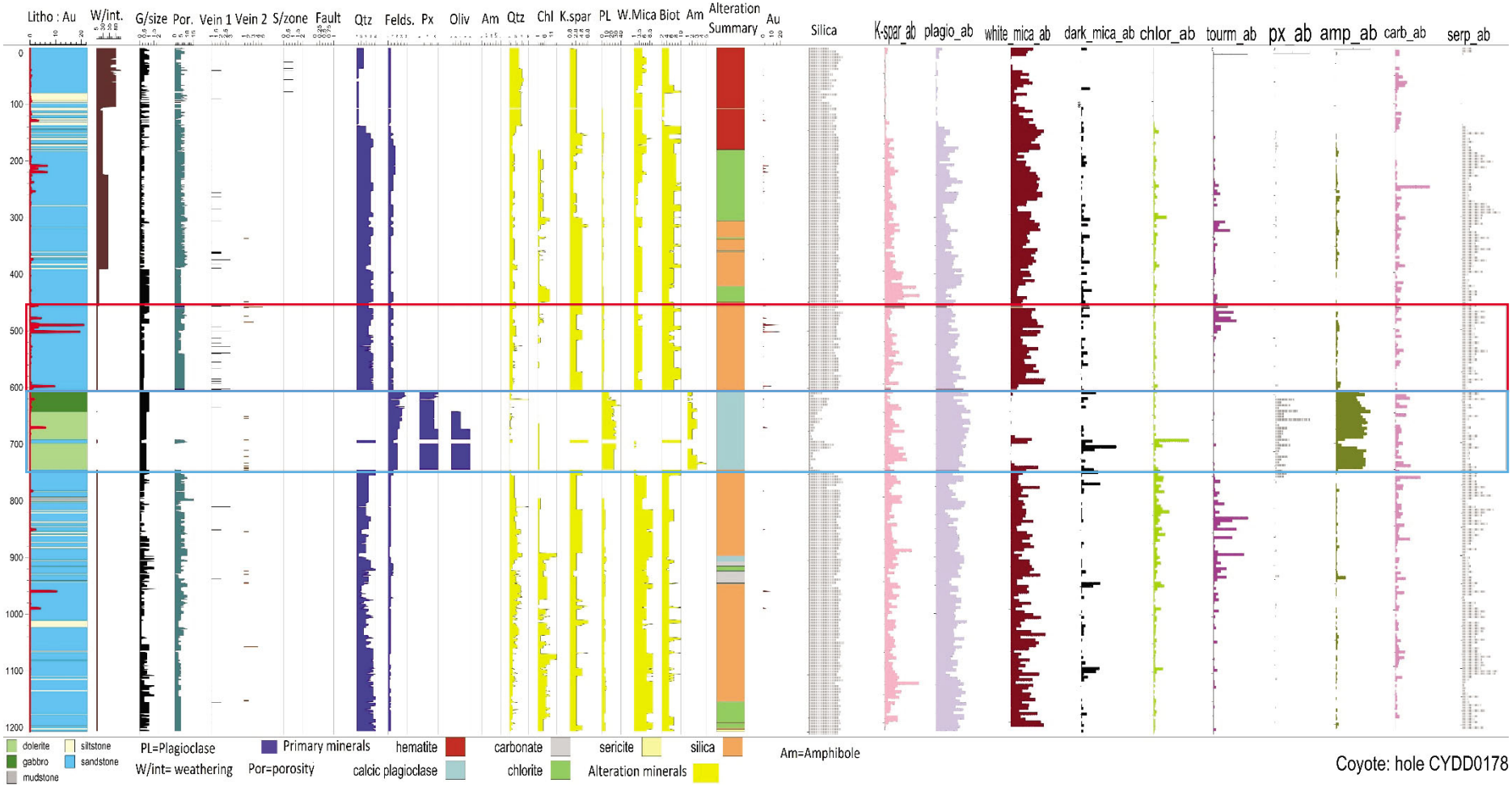

Figure 11 c). Integrated Coyote graphic and spectral logs.

4) Petrographic data analysis

Ten samples were collected from CYDD0178 and submitted to MINEREX Laboratory Service in Kalgoorlie, WA, for preparation of ten thin sections. The samples were mainly collected from Type I and Type II Veins and wall rocks from intersections of anticline and fault zones. Petrographic observations were used in conjunction with geochemical data; hyperspectral data; conventional log, and additional geological observations from literature with the aim of establishing the chronology of events for Coyote gold deposit.

I. Type I Veins

Five thin sections of mineralised veins from sandstone, siltstone, gabbro, and dolerite host rocks were examined.

The veins consist of more than 60% quartz that are moderate to intensely deformed, as distinguished by undulose extinction in crossed polarised light, and 5% calcite. These veins also display parallel elongated quartz – filled fractures that are dominantly associated with pyrite and pyrrhotite. Two sets of veins cross-cut each other; one is mineralised and is associated with pyrrhotite. This is interpreted as vein type 1b, probably linked to second deformation event (DGTO2). This vein is precipitated as quartz along fractured vein type 1a. Further, folded quartz vein in which pyrrhotite replaces pyrite was recognised as well. The pyrrhotite is strongly anisotropic and seen as hexagonal crystals, whereas, pyrite is isotropic.

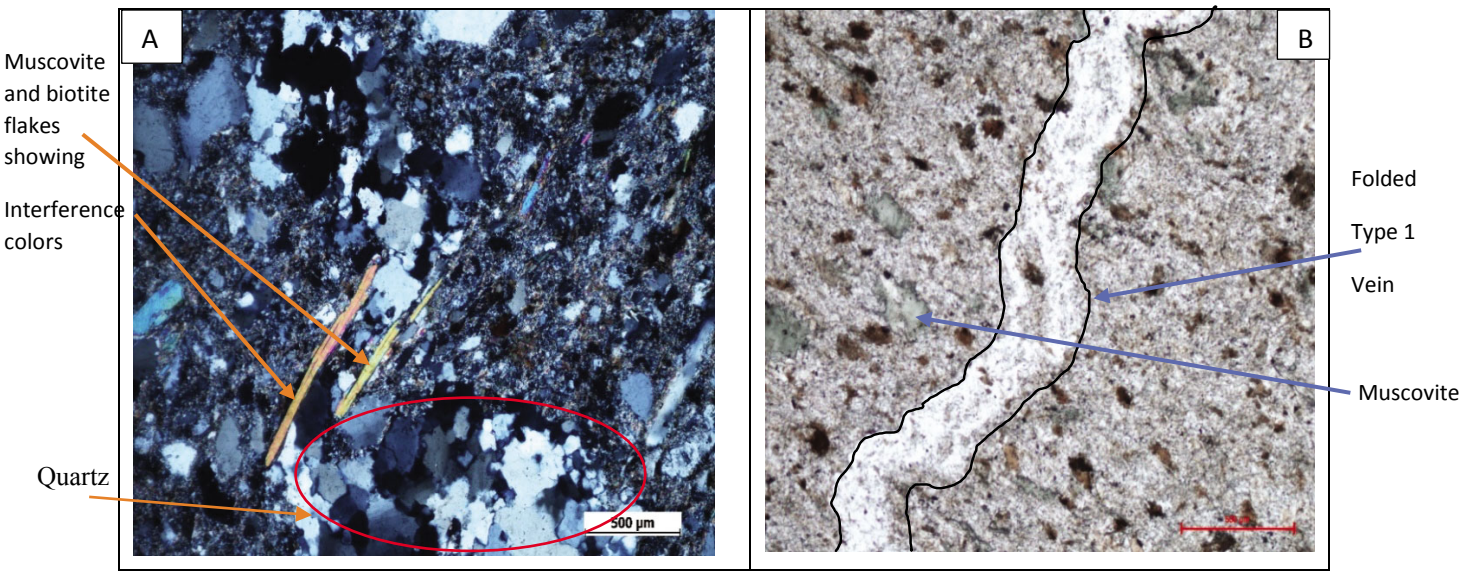

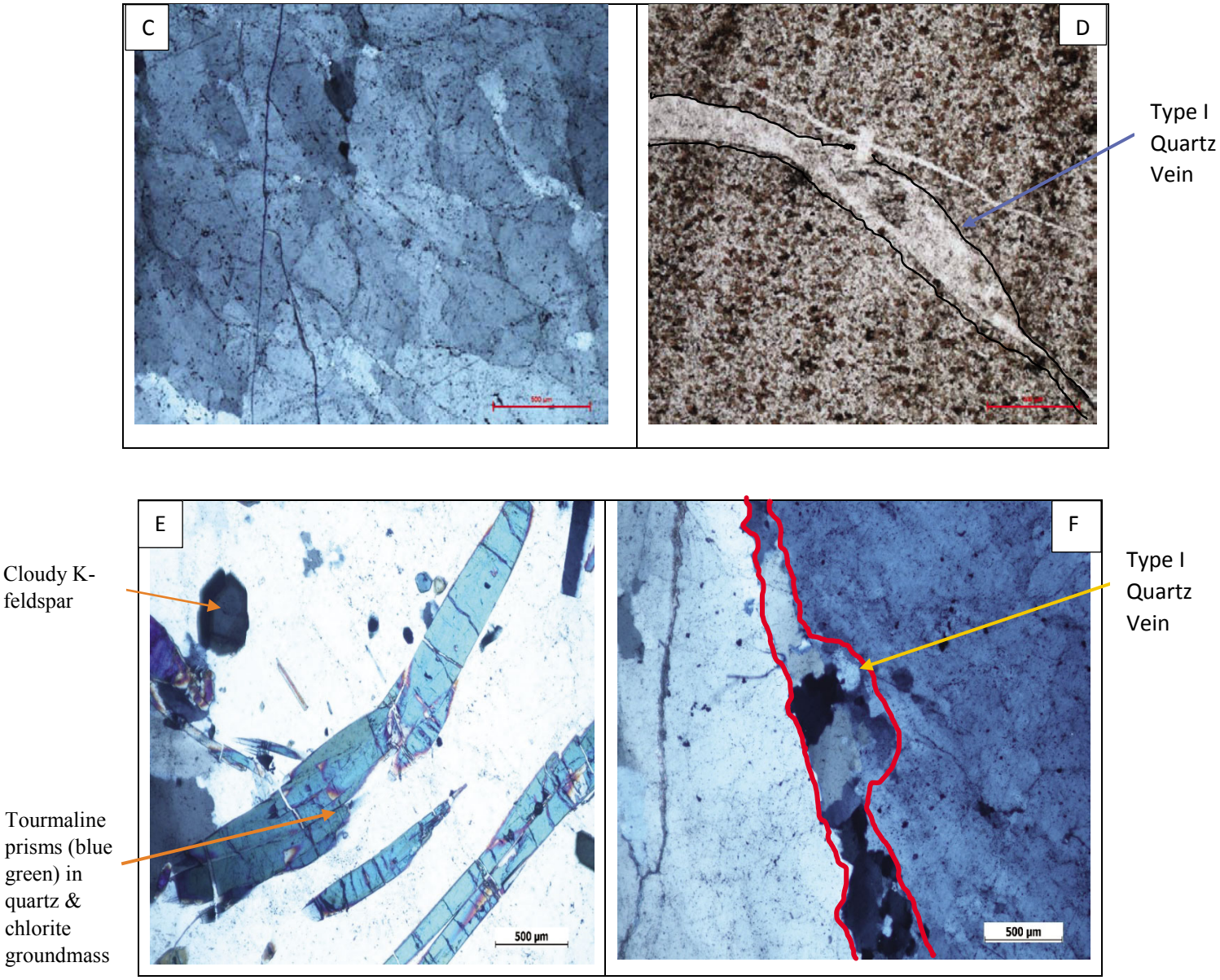

Figure 12. Photomicrographs of Type I veins A) euhedral quartz associated with pyrite and arsenopyrite B) Folded bedding-parallel vein associated with pyrite, chalcopyrite, and galena C) gabbro-hosted quartz veinlets surrounded by crystals of plagioclase, augite, and biotite - visible gold associated with pyrite and pyrrhotite D) parallel veins associated with carbonate, pyrite and pyrrhotite E) tourmaline crystals in quartz and chlorite groundmass, and F) dolerite-hosted fracture-filling style of mineralisation, mainly associated with biotite, pyrite and pyrrhotite.

Mineralisation is variably associated with pyrite, chalcopyrite, pyrrhotite, arsenopyrite, and minor sphalerite and galena displaying triangular pits texture. The pyrite is variably fine grained, disseminated, anhedral and euhedral crystals, commonly precipitated along fractures.

In addition to sulfides, associated gangue minerals include 5 – 10% of light-medium green chlorite, occurring along fractures, and associated with sulfides, 5 – 7% K-feldspar, 5 -10%

minor amounts of tourmaline, hornblende, augite, calcic plagioclase, hematite. Mineralisation style is commonly fracture/vein filling in shear zones and are associated with intense silica – chlorite alteration style.

II. Type II Veins

Two thin sections of Type II veins (bucky quartz) from silicified sandstone and siltstone were studied. The veins are composed of milky quartz that are sheared, silicified, and fractured. Gangue minerals include quartz, muscovite, chlorite, biotite, k-feldspar, brown hornblende, and plagioclase. Large euhedral crystals of arsenopyrite are deposited along quartz grain boundaries and in fractures where they are associated with pyrrhotite.

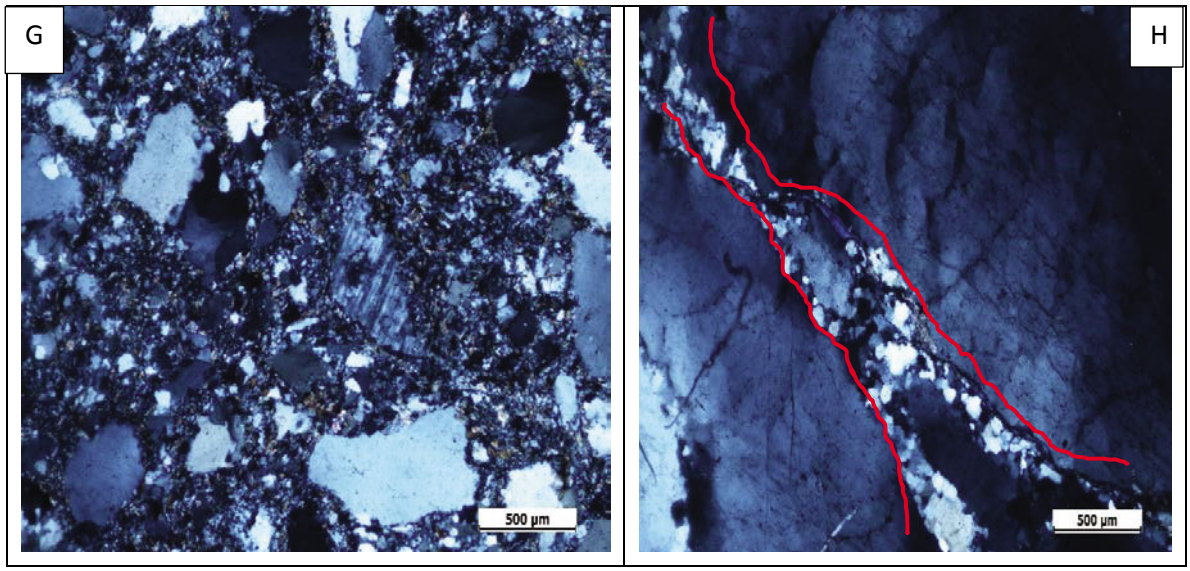

Figures 12. Photomicrographs under XPL G) Sandstone-hosted barren quartz associated with calcite H) Bedding parallel barren quartz vein, solid red lines represent main vein associated with large euhedral porphyritic arsenopyrite and disseminated pyrrhotite precipitated along quartz grain boundaries and in fractures.

III. Wall rocks from intersecting Anticline and Fault zone

Three thin sections of wall rock from intersecting structures were analysed to characterise these structures. Gangue minerals are highly deformed and these include sheared quartz, muscovite, chlorite, and biotite. The intersecting structures display intense silica – chlorite

alteration. Mineralisation style is vein filling and is associated with idiomorphic, and fractured pyrite, and arsenopyrite.

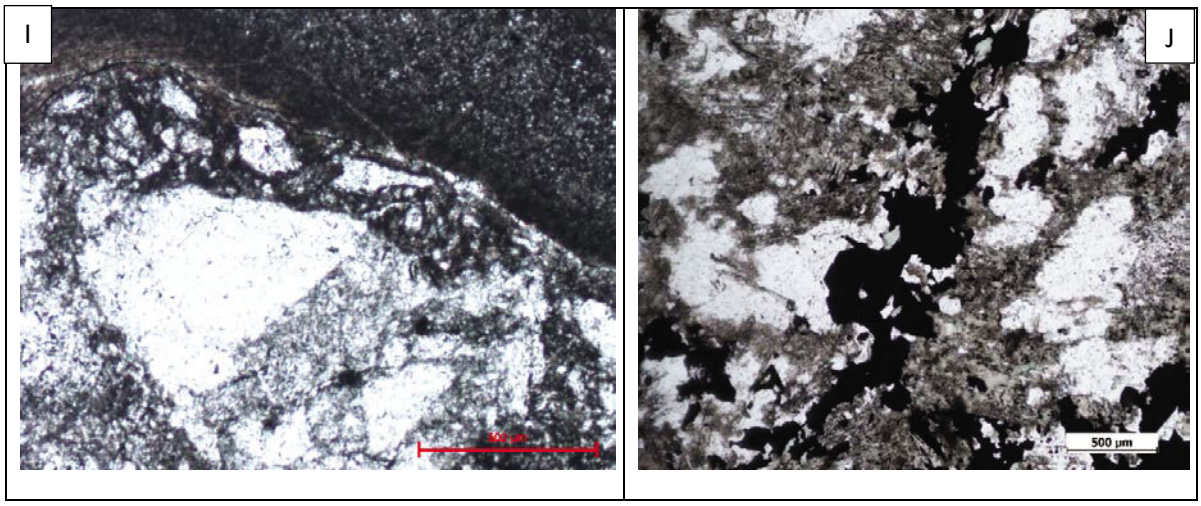

Figure 12. photomicrographs of I) Intensely deformed and chlorite-biotite-quartz-dominated sandstone J) Intensely sheared/deformed quartz vein associated with intense silica-chlorite alteration.

IV. Chronology of geologic events at Coyote deposit

a) Paragenetic sequence of characteristic alteration assemblages at Coyote deposit, WA.

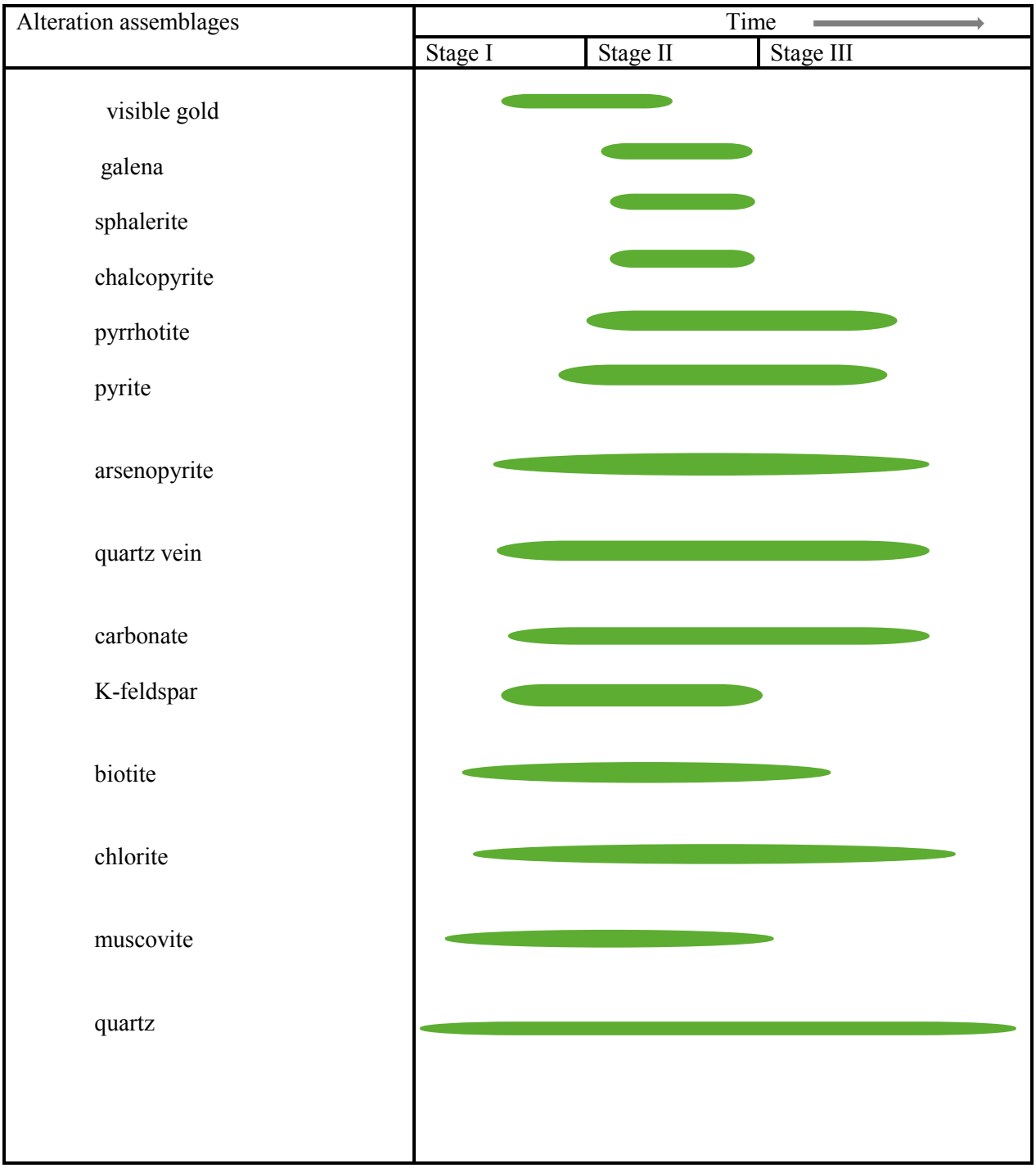

Figure 13. a) Paragenetic Sequence of characteristic alteration assemblages at Coyote deposit.

Sulfides phases

Three stages of sulphides paragenesis have been recognised at Coyote deposit. The first stage is characterised by disseminated crystals of arsenopyrite and pyrrhotite. This is accompanied by introduction of pyrite, pyrrhotite, chalcopyrite and minor sphalerite and galena. Both the first and second stages are associated with gold mineralisation. The third stage is associated with introduction of large crystals of arsenopyrite and disseminated pyrite.

b) Interpreted Paragenetic sequence of Coyote deposit, WA.

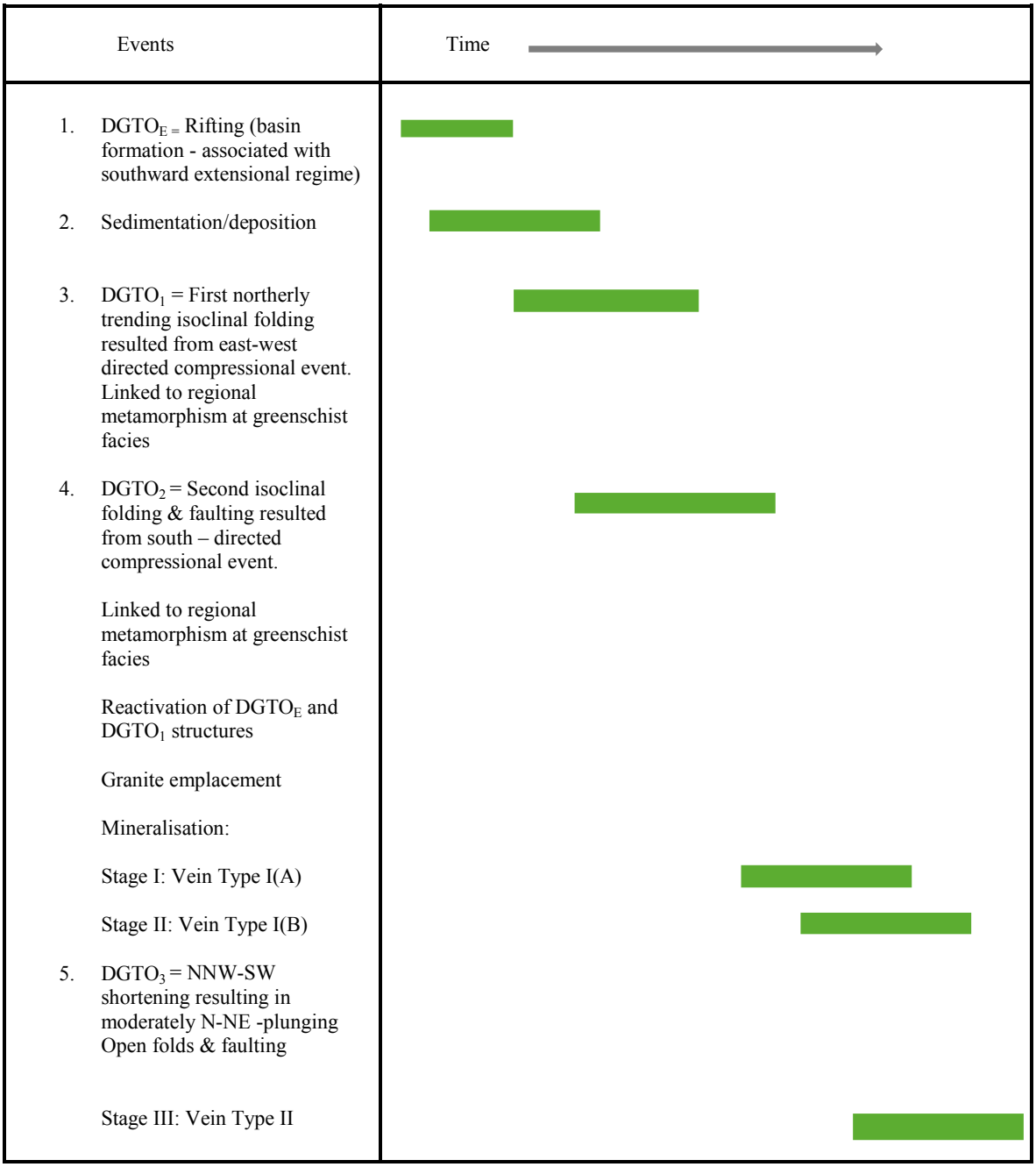

Figure 13. b) Interpreted Paragenetic Sequence of Coyote deposit, WA.

5) Discussions

I. Local controls on alterations and mineralisation

a) Nature of host rocks

The results obtained from logging, assay data, hyLogger data, and petrography suggest that the influence of host rock at Coyote deposit stemmed from factors such as mineral composition, grain size, texture, porosity and permeability, and foliation. Sandstone layers which are primarily composed of quartz, alkali feldspar, plagioclase, and muscovite, are principally characterised by silicification and iron-rich sulfides (pyrite and pyrrhotite) and minor sphalerite and galena. Dolerite and gabbro, in contrast, are associated with chlorite, carbonate, and iron-rich sulfides (pyrite and pyrrhotite). These mafic rocks mainly comprise pyroxenes, plagioclase, and hornblende. Furthermore, grain size controls porosity and permeability of host rocks. Permeability is important because it enhances fluid motion through the host rocks. Logging has indicated that the sandstone and dolerite rocks are medium to coarse grain, and are associated with moderate porosity. Clearly, logging and analyses of CYDD0178 have shown that sandstone and dolerite are the most favourable host rocks for gold mineralisation and this is attributed in parts to their mineralogical and textural characteristics.

b) Competency contrast

The control of rheological difference in host rocks on the mineralised structures is evidenced by abundant mineralisation in shear zones along stratigraphic contacts and restriction of vein-style mineralisation to competent lithologies. At Coyote deposit, rheological difference between the more competent sandstone beds and the less competent siltstone and mudstone layers have resulted in creation of dilatational sites favourable for deposition of gold-rich fluids.

II. Regional control on alterations and mineralisation

Regional controls on Coyote gold mineralisation is a product of interactions between deformation events, low grade regional metamorphism, and magmatism. Deformation events are responsible for creation of crustal-scale/mantle tapping structures that provides conduits and traps for transportation and localisation of gold-rich quartz veins. Evidence suggests that

gold mineralisation at Coyote is located in intersecting structures. Given that the Gonzales Fault and Coyote anticlinal fold are linked to $DGTO_2$ episode (e.g., Bagas et al., 2009), such association suggests that regional deformation event controls gold mineralisation. Furthermore, regional deformation episodes, low grade metamorphism and the associated metamorphic assemblages are interrelated.

III. Intrusion-related vs orogenic gold model

Poorly-defined deposits model often result in unsuccessful exploration plan (Hart, 2005). Hence, differentiating between closely similar intrusion-related and orogenic vein gold deposits is crucial for a successful gold exploration program (e.g., Sillitoe and Thompson, 1998; Buchholz et al., 1998; Qiu and McNaughton 1999; Lang et al., 2001; Robert 2001).

Orogenic gold deposits are widely defined as deposits formed from crustal-scale fluids derived through metamorphic devolatisation during or immediately after compressive deformation and regional metamorphism (e.g., Philips and Powell, 1993; Goldfarb et al., 1998; Groves et al., 1998, Stuwe 1998). Intrusion-related gold deposits on the other hand, are defined as a class of deposits characterised by diverse mineralisation styles, granitoid association and accretionary and collisional tectonic settings (Sillitoe, 1991; Hart, 2005, and Thompson et al., 1999). A range of mineralisation styles include porphyry, breccia, skarn, replacement and vein types (e.g., Sillitoe, 1991), however, the gold-rich vein types are ambiguous in terms of genetic classification because of their similarity to orogenic gold deposits (Groves et al., 1989; Kerrich, 1991; Hodgson, 1993).

A set of distinguishing features that characterises Coyote gold deposit are listed below. These characteristics were compared with features of Reduced intrusion-related class (Hart et al., 2004b) to support intrusion-related origin.

i) Tectonic setting: mineralisation associated with intrusions that were emplaced into Paleoproterozoic collisional orogens and hosted in metasedimentary rocks.
ii) Metal zoning: associated with elevated Au-Bi-Te-As-Ag-K-Pb-Al assemblage.
iii) Deposits styles: country-rock hosted consisting of replacements, and veins. Gold mineralisation characterised by a wide range of gold grades.
iv) Sheeted Veins: sheeted arrays of parallel, low-sulphide content except large arsenopyrite crystals, fluid exsolution, and quartz and tourmaline veins.
v) Redox state: associated with felsic, ilmenite-series plutons that lack magnetite have low magnetic susceptibilities.

vi) Timing: gold mineralisation is synchronous with granite emplacement.

Goldfarb et al. (2000) emphasise the significance of metal assemblages in the veins, the presence of K-feldspar as indicator of magmatic source for the auriferous fluid. Orogenic gold deposits are characterised by strong sericite-ankerite-carbonate alteration, and K-feldspar alteration is generally low to absent (Lang et al., 2001). Coyote deposit display significant enrichment in albite, a feature not typical of orogenic gold deposit.

Furthermore, the gold-rich veins are associated with base metal sulfides such as galena and sphalerite. According to Goldfarb et al. (2000), the reduced intrusion-related gold system form veins that are enriched in base metals, a feature not common in orogenic gold deposits (Goldfarb et al., 2000).

Additionally, geochemical analyses have shown that higher gold grades strongly correlate with Bi. Several authors (Baker., 1996 F; Pollard., 1985 F; Mark and Mustard 1999; and Graham 2005), have suggested that the link between Au and Bi may provide clues into the source and precipitation mechanisms. Such association suggests different sources for Bi and Au, or deposition under similar conditions (Baker., 1996 F; Pollard., 1985 F; Mark and Mustard 1999; and Graham 2005). Mustard and Ulrich (2004) propose that the Au probably originated from primitive magmas but is concentrated by the same differentiation mechanism that concentrated Bi. Douglas et al. (2000) have illustrated the significance of Bi in scavenging Au from a hydrothermal fluid through their liquid bismuth collector model. Thus, if Au is present in reduced, granite-derived fluids, it will most likely be associated with Bi.

Key Findings of investigations of diamond drill hole CYDD0178

i) Two major Formations of the Tanami Group; the Killi Killi and the Stubbins Formations have been intersected. The stratigraphic succession is dominated by interbedded sandstone, siltstone, and carbonaceous mudstone and shale beds, intruded by dolerite and gabbro sills.

ii) Hydrothermal alterations and gold localisation are influenced in part by nature of host rocks such as grain size, mineral composition, foliation, shearing, porosity, and permeability. Geochemical data analysis has shown that majority of gold is hosted in the sandstone and dolerite units.

iii) Gold is localised in fractures in shear zones and along grain boundaries suggesting that the intersecting structures are the most favourable depositional sites. In this case, the Gonzales Fault and the Coyote Anticlinal Fold have acted as damaged high permeability zones suitable for transfer and precipitation of auriferous fluids. Hence, structures are the most significant controls which not only influenced the flow of hydrothermal fluids, but granite emplacement as well.

iv) Rheological differences between sandstone beds and siltstone layers have created dilatational sites along stratigraphic contacts favourable for precipitation of gold-laden fluid.

v) Two types of quartz veins have been categorised; Type I (a) and (b), and Type II veins. Type I is the economic vein whereas Type II is barren quartz.

vi) Vein assemblages include Type I (a) quartz-albite-chlorite-biotite-tourmaline-calcite-pyrite-arsenopyrite, and visible Au; Type I (b) quartz-albite-biotite-chlorite-tourmaline-carbonate-pyrite-pyrrhotite-arsenopyrite-chalcopyrite-galena-sphalerite, and visible Au; and Type II include carbonate-arsenopyrite-pyrrhotite.

vii) High grade gold corresponds to high vein density zones suggesting that mineralisation is structurally controlled.

viii) Vectors to Ore (pathfinders) include Au with elevated Bi-Te-As-Ag-Pb suite.

ix) Low sulfides content that encompasses arsenopyrite-pyrite-pyrrhotite-chalcopyrite-galena-sphalerite assemblage, and wide range of gold grades of 21.025, 19.407, 10.385, 6.08, 3.984, and 1.6 (in ppm).

x) Gold mineralisation is synchronous with regional deformation episode (DGTO2), and granite emplacement.

xi) Gold is probably sourced from two basic sources: i) country rock through metamorphic devolatisation, and ii) released by cooling pluton.

xii) Data and observations suggest that Coyote deposit lies between intrusion-related and orogenic gold models. This paper argues that the gold was sourced from both the magma and country rock. However, magma is the principal driver of energy and fluids that scavenged some gold from the host rock.

Acknowledgment

The author would like to thank the Geological Survey of Western Australia, Perth, for their substantial contribution towards the success of this work. Similarly, my sincere appreciation goes to my supervisors Dr. Sandra Occhipinti, Dr. Alan Aitken, and Dr. Paul Duuring for their constant guidance throughout the course of this research project.

REFERENCES

Adams, G. J., Both, R. A., & James, P. (2007). The Granites gold deposits, Northern Territory, Australia: evidence for an early syn-tectonic ore genesis. *Mineralium Deposita, 42*(1-2), 89-105.

Bagas, L., Anderson, J., & Bierlein, F. (2009). Palaeoproterozoic evolution of the Killi Killi Formation and orogenic gold mineralization in the Granites–Tanami Orogen, Western Australia. *Ore Geology Reviews, 35*(1), 47-67.

Bagas, L., Boucher, R., Li, B., Miller, J., Hill, P., Depauw, G. Eggers, B. (2014). Paleoproterozoic stratigraphy and gold mineralisation in the Granites-Tanami Orogen, North Australian Craton. *Australian Journal of Earth Sciences, 61*(1), 89-111.

Bagas, L., Huston, D. L., Anderson, J., & Mernagh, T. P. (2007). Paleoproterozoic gold deposits in the Bald Hill and Coyote areas, western Tanami, Western Australia. *Mineralium Deposita, 42*(1-2), 127-144.

Blake, D., & McDougall, I. (1973). Ages of the Cape Hoskins volcanoes, New Britain, Papua New Guinea. *Journal of the Geological Society of Australia, 20*(2), 199-204.

Blake, D. H., Hodgson, I. M., & Muhling, P. C. (1979). *Geology of The Granites-Tanami Region, Northern Territory and Western Australia* (Vol. 197): Australian Government Publishing Services.

Buchholz, P., Herzig, P., Friedrich, G., & Frei, R. (1998). Granite-hosted gold mineralization in the Midlands greenstone belt: a new type of low-grade gold deposit in Zimbabwe. *Mineralium Deposita, 33*(5), 437-460.

Christie, A. B., & Brathwaite, R. L. (2003). Hydrothermal alteration in metasedimentary rock-hosted orogenic gold deposits, Reefton goldfield, South Island, New Zealand. *Mineralium Deposita, 38*(1), 87-107.

Clark, R. N., & Roush, T. L. (1984). Reflectance spectroscopy: Quantitative analysis techniques for remote sensing applications. *Journal of Geophysical Research: Solid Earth, 89*(B7), 6329-6340.

Cox, S., Knackstedt, M., & Braun, J. (2001). Principles of structural control on permeability and fluid flow in hydrothermal systems. *Reviews in Economic Geology, 14*, 1-24.

Crispe, A., Vandenberg, L., & Scrimgeour, I. (2007). Geological framework of the Archean and Paleoproterozoic Tanami Region, Northern Territory. *Mineralium Deposita, 42*(1-2), 3-26.

Cross, A., & Crispe, A. (2007). SHRIMP U–Pb analyses of detrital zircon: a window to understanding the Paleoproterozoic development of the Tanami Region, northern Australia. *Mineralium Deposita, 42*(1-2), 27-50.

Cudahy, T., Jones, M., Thomas, M., Laukamp, C., Caccetta, M., Hewson, R., . . . Verrall, M. (2008). Next generation mineral mapping: Queensland airborne HyMap and satellite ASTER surveys 2006–2008. *Commonwealth Scientific and Industrial Research Organization Report*.

Goldfarb, R., Groves, D., & Gardoll, S. (2001). Orogenic gold and geologic time: a global synthesis. *Ore Geology Reviews, 18*(1), 1-75.

Goleby, B. R., Huston, D. L., Lyons, P., Vandenberg, L., Bagas, L., Davies, B. M., . . . Smith, T. (2009). The Tanami deep seismic reflection experiment: An insight into gold mineralization and Paleoproterozoic collision in the North Australian Craton. *Tectonophysics, 472*(1), 169-182.

Griffin, T., Page, R., Sheppard, S., & Tyler, I. (2000). Tectonic implications of Palaeoproterozoic post-collisional, high-K felsic igneous rocks from the Kimberley region of northwestern Australia. *Precambrian Research, 101*(1), 1-23.

Groves, D., Barley, M. E., & Ho, S. E. (1989). Nature, genesis, and tectonic setting of mesothermal gold mineralization in the Yilgarn Block, Western Australia. *Econ Geol Monogr, 6*, 71-85.

Hancock, E., & Huntington, J. F. (2010). *The GSWA NVCL HyLogger: rapid mineralogical analysis for characterizing mineral and petroleum core*: Geological Survey of Western Australia.

Hart, C., & Goldfarb, R. (2005). *Distinguishing intrusion-related from orogenic gold systems.* Paper presented at the New

Zealand Minerals Conference Proceedings.

Hart, C. J. (2005). Classifying, distinguishing and exploring for intrusion-related gold systems. *The Gangue, 87*, 3-9.

Hart, C. J., Mair, J. L., Goldfarb, R. J., & Groves, D. I. (2004). Source and redox controls on metallogenic variations in intrusion-related ore systems, Tombstone-Tungsten Belt, Yukon Territory, Canada. *Geological Society of America Special Papers, 389*, 339-356.

Hillyard, C. (2012). Coyote Deeps diamond hole final report.

Hodgson, C. (1993). Mesothermal lode-gold deposits. *Mineral Deposit Modelling. Edited by RV Kirkham, WD Sinclair, RI Thorpe and JM Duke. Geological Association of Canada, Special Paper, 40*, 635-678.

Huston, D. L. (2006). *Mineral systems and tectonic evolution of the North Australian Craton.* Paper presented at the Evolution and metallogenesis of the North Australian Craton, Conference Abstracts. Geoscience Australia Record.

Huston, D. L., Vandenberg, L., Wygralak, A. S., Mernagh, T. P., Bagas, L., Crispe, A., . . . Williams, N. (2007). Lode–gold mineralization in the Tanami region, northern Australia. *Mineralium Deposita, 42*(1-2), 175-204.

Joly, A., McCuaig, T. C., & Bagas, L. (2010). The importance of early crustal architecture for subsequent basin-forming, magmatic and fluid flow events. The Granites-Tanami Orogen example. *Precambrian Research, 182*(1), 15-29.

Joly, A., Porwal, A., & McCuaig, T. C. (2012). Exploration targeting for orogenic gold deposits in the Granites-Tanami Orogen: mineral system analysis, targeting model and prospectivity analysis. *Ore Geology Reviews, 48*, 349-383.

Kerrich, R. (1991). Radiogenic isotope systems applied to mineral deposits. *Short course handbook on applications of radiogenic isotope systems to problems in geology/Heaman L., Ludden JN (eds). Min. Assoc. Canada, Toronto*, 365-421.

Lambeck, A., Huston, D., Maidment, D., & Southgate, P. (2008). Sedimentary geochemistry, geochronology and sequence stratigraphy as tools to typecast stratigraphic units and constrain basin evolution in the gold mineralised Palaeoproterozoic Tanami Region, Northern Australia. *Precambrian Research, 166*(1), 185-203.

Lang, J. R., & Baker, T. (2001). Intrusion-related gold systems: the present level of understanding. *Mineralium Deposita, 36*(6), 477-489.

Laukamp, C., Cudahy, T., Caccetta, M., Chia, J., Gessner, K., Haest, M., . . . Rodger, A. (2010). The uses, abuses and opportunities for hyperspectral technologies and derived geoscience information. *AIG Bull., 51*, 73-76.

Li, B., Bagas, L., Gallardo, L. A., Said, N., Diwu, C., & McCuaig, T. C. (2013). Back-arc and post-collisional volcanism in the Palaeoproterozoic Granites-Tanami Orogen, Australia. *Precambrian Research, 224*, 570-587.

Mustard, R., Mark, G., Ulrich, T., Gillen, D., & Foster, D. Geochemistry of magmatic fluids from intrusions of the Williams-Naraku Batholith, Cloncurry District, Northwest Queensland: preliminary results from laser ablation ICP-MS analysis.

Nude, P. M., Asigri, J. M., Yidana, S. M., Arhin, E., Foli, G., & Kutu, J. M. (2012). Identifying pathfinder elements for gold in multi-element soil geochemical data from the Wa-Lawra belt, northwest Ghana: a multivariate statistical approach. *International Journal of Geosciences, 3*(01), 62.

Oliver, N. H., & Bons, P. D. (2001). Mechanisms of fluid flow and fluid–rock interaction in fossil metamorphic hydrothermal systems inferred from vein–wallrock patterns, geometry and microstructure. *Geofluids, 1*(2), 137-162.

Phillips, G. N., & Powell, R. (1993). Link between gold provinces. *Economic Geology, 88*(5), 1084-1098.

Pirajno, F., & Bagas, L. (2008). A review of Australia's Proterozoic mineral systems and genetic models. *Precambrian Research, 166*(1), 54-80.

Qiu, Y., & Groves, D. I. (1999). Late Archean collision and delamination in the Southwest Yilgarn Craton; the driving force for Archean orogenic lode gold mineralization? *Economic Geology, 94*(1), 115-122.

Ridley, J., & Mengler, F. (2000). Lithological and structural controls on the form and setting of veins stockwork orebodies at the Mount Charlotte gold deposit, Kalgoorlie. *Economic Geology, 95*(1), 85-98.

Robert, F., Boullier, A. M., & Firdaous, K. (1995). Gold-quartz veins in metamorphic terranes and their bearing on the role

of fluids in faulting. *Journal of Geophysical Research: Solid Earth, 100*(B7), 12861-12879.

Robert, F., & Poulsen, K. H. (2001). Vein formation and deformation in greenstone gold deposits. *Reviews in Economic Geology, 14*, 111-155.

Sillitoe, R. (1991). Intrusion-related gold deposits *Gold metallogeny and exploration* (pp. 165-209): Springer.

Sillitoe, R. H. (2000). Gold-rich porphyry deposits: descriptive and genetic models and their role in exploration and discovery. *Reviews in Economic Geology, 13*, 315-345.

SILLITOE, R. H., & THOMPSON, J. F. (1998). Intrusion–Related Vein Gold Deposits: Types, Tectono-Magmatic Settings and Difficulties of Distinction from Orogenic Gold Deposits. *Resource Geology, 48*(4), 237-250.

Stevenson, D., Bagas, L., Aitken, A., & McCuaig, T. (2013). A geophysically constrained multi-scale litho-structural analysis of the Trans-Tanami Fault, Granites-Tanami Orogen, Western Australia. *Australian Journal of Earth Sciences, 60*(8), 745-768.

Stüwe, K. (1998). Tectonic constraints on the timing relationships of metamorphism, fluid production, and gold-bearing quartz vein emplacement. *Ore Geology Reviews, 13*(1), 219-228.

Tunks, A. J., & Cooke, D. R. (2007). Geological and structural controls on gold mineralization in the Tanami District, Northern Territory. *Mineralium Deposita, 42*(1-2), 107-126.

Williams, N. (2007). Controls on mineralisation at the world-class Callie gold deposit, Tanami desert, Northern Territory, Australia. *Miner Deposita, 42*, 65-87.

Wygralak, A. S., Mernagh, T., Huston, D. L., & Ahmad, M. (2005). *Gold mineral system of the Tanami Region*: Government Printer, South Africa.

Young, D., Fanning, C., Shaw, R., Edgoose, C., Blake, D., Page, R., & Camacho, A. (1995). U-Pb zircon dating of tectonomagmatic events in the northern Arunta Inlier, central Australia. *Precambrian Research, 71*(1-4), 45-68.

Online Appendix 1 Coyote Drillhole CYDD0178 log (Excel Spreadsheet CoyoteDrillHoleCYDD0178Log.xls)

RECORD 2017/12

CONTROLS ON HYDROTHERMAL ALTERATIONS AND GOLD MINERALISATION AT COYOTE DEPOSIT, WESTERN AUSTRALIA

RoI

This Record is published in digital format (PDF) and is available as a free download from the DMIRS website at <www.dmp.wa.gov.au/GSWApublications>.

Further details of geological products produced by the Geological Survey of Western Australia can be obtained by contacting:

Information Centre
Department of Mines, Industry Regulation and Safety
100 Plain Street
EAST PERTH WESTERN AUSTRALIA 6004
Phone: +61 8 9222 3459 Fax: +61 8 9222 3444
www.dmp.wa.gov.au/GSWApublications